Closed Loop Guidance of Jovian Moon Orbiter Mission Using Space Manifold Dynamics

Thesis Report

Submitted in partial fulfillment of the requirements for the award of M.Tech Degree in Electrical Electronics Engineering (Guidance And Navigational Control) of the University of Kerala

Submitted by

Arun Suresh
M.Tech
Guidance And Navigational Control
Reg No: 13400007

Department of Electrical Engineering
College of Engineering Trivandrum
Thiruvananthapuram-16
2015

Department of Electrical Engineering
College of Engineering, Trivandrum
Thiruvananthapuram-16
2015

Certificate

This is to certify that this report entitled **"Closed Loop Guidance of Jovian Moon Orbiter Mission Using Space Manifold Dynamics"** *is a bonafide record of the Thesis work done by* **Arun Suresh** *of* 3^{rd} Semester, M.Tech *under our guidance towards the partial fulfillment of the requirements for the award of* **M.Tech Degree** *in* **Electrical and Electronics Engineering** *of the* **University of Kerala** *during the year 2014.*

Dr. W C Arunkishore
Associate Professor
((Dept. of Electrical Engineering))
College of Engineering, Trivandrum
(Internal Guide)

Dr U P Rajeev
Head
(CGDG/CGSE)
VSSC Trivandrum
(External Guide)

Dr. S Ushakumari
P G Cordinator
Department of Electrical Engineering
College of Engineering, Trivandrum

Dr. B Ajith Kumar
Head of Department
Department of Electrical Engineering
College of Engineering, Trivandrum

Acknowledgement

I have great pleasure in expressing my gratitude and obligations to **Dr Rajeev U P**,Head, CGDG/CGSE, VSSC Trivandrum, for his exemplary guidance, monitoring and constant encouragement throughout the course of this thesis. I am thankful for his aspiring guidance, invaluably constructive criticism and friendly advice during the work. I am sincerely grateful to him for sharing his truthful and illuminating views on a number of issues related to the project. The blessing, help and guidance given by him time to time shall carry me a long way in the journey of life on which I am about to embark.

I express my thanks to **Dr. Arun Kishore W. C**,Associate Professor , Department of Electrical Engineering, College of Engineering, Trivandrum, who has continually and persuasively conveyed a spirit of adventure in regard to research, and an excitement in regard to teaching. Without his supervision and constant help this dissertation would not have been possible.

I express my gratitude to **Dr. B Ajith Kumar**, Professor & Head of the Department, Department of Electrical Engineering, College of Engineering, Trivandrum for his support and guidance.

Furthermore I would like to thank **Chandana Chandran** for introducing me to the topic as well for the support on the way.

I also acknowledge my gratitude to other members of faculty in the Department of Electrical Engineering, my family and friends for their whole hearted cooperation and encouragement. Above all, I thank GOD Almighty, without whose help, I wouldn't have reached this far.

Trivandrum **Arun Suresh**

Abstract

New three body perspectives are used to design successful and efficient missions which take full advantage of the natural dynamics, and are used for design of low energy trajectories. This work proposes a closed loop guidance algorithm using space manifold dynamics. A Single Spacecraft is designed to orbit 2 Galilean moons of Jupiter, Ganymede and Europa. Europa is thought to be a hospitable to life because of vast liquid ocean that may exist under its icy crust. Mission Employs dynamical channels in the phase space (tubes in the energy surface which naturally link the vicinity of Ganymede to the vicinity of Europa). By approximating the dynamics of the Jupiter-Europa- Ganymede-spacecraft 4 -body problem as two 3 body sub problems, the intersections between stable and unstable manifold tubes of different moons are obtained. The transfer Δv necessary to jump from one moon to another is less than that required by a standard Hohmann transfer. The system is nonlinear and highly dependent on initial conditions. Dynamic equations are obtained and a controller based on the dynamic inverse is synthesized for the purpose of stabilization and trajectory tracking.

Contents

List of Figures

List of Tables

NOTATIONS

Notations	Meaning
x,y,z	Position Cordinates in Rotating Frame
X,Y,Z	Position Cordinates in Inertial Frame
$\dot{x}$,$\dot{y}$,$\dot{z}$	x Velocity in Rotating Frame
$\dot{X}$,$\dot{Y}$,$\dot{Z}$	x Velocity in Rotating Frame
μ	Gravitational Parameter
Ω	Potential Function
C	Jacobi Integral
E	Total Energy
G	Gravitational Constant
ω	Angular Velocity

Chapter 1

INTRODUCTION

Europa is one of Galilean Moons of Jupiter, where possible subterranean oceans and life are suspected. There has been significant interest in sending a scientific spacecraft to orbit and study Europa. One of the main difficulties with such a mission is the construction of a feasible trajectory from the Earth to Europa using a very limited fuel budget. One must take full advantage of the orbital dynamics in order to find even a reasonable first guess at such a trajectory. New three-body perspectives are required to design successful and efficient missions which take full advantage of the natural dynamics. Not only does a three-body approach provide low-fuel trajectories, but it also increases the flexibility and versatility of missions.Fortunately, Jupiter's vicinity, and in particular the Galilean moons, provide enough interesting orbital dynamics that the construction of a relatively low fuel trajectory is possible. A trajectory is designed which ends in ballistic capture at Europa and beforehand executes a temporary capture around Ganymede. The spacecraft can circle a moon in a loose temporary capture orbit for a desired number of orbits, perform a transfer ΔV and become ballistically captured by another adjacent moon for some number of orbits, etc. Instead of flybys lasting only seconds, a scientific spacecraft can orbit several different moons for any desired duration.

Taking full advantage of the N-body dynamics of a system, the fuel necessary to

transfer between moons can be significantly less than that required by a Hohmann transfer. This is essentially due to the brute force nature of the Hohmann transfer which approximates each leg of the trajectory locally by 2-body solutions. The transfer ΔV is almost half the Hohmann transfer value.

Traditional mission design focused on a model of the system that is consistent with the two-body problem, usually comprised of some massive central body and a much less massive spacecraft. Ultimately, this approach lead to spacecraft equations of motion that result in the conic sections of Keplerian motion. The gravitational fields of any additional bodies were then modelled as perturbations to the conic solution. Preliminary analysis for more ambitious missions was accomplished through a sequence of two-body arcs linked via the "patched conic" method. A more general formulation of the problem that incorporates one additional gravitational interaction could be modelled as three-body problem in orbital mechanics. Unlike the two body problem, there is no closed form analytical solution for the differential equations governing the motion in the three-body problem. However, it is still possible to gain insight into the qualitative nature of the solutions in this system when several simplifying assumptions were introduced. This reduced model is denoted as the restricted three-body problem. The problem was further simplified by constraining the primaries to move in circular orbits about their center of mass. The resulting simplified model was labelled as the circular restricted three-body problem (CR3BP). Although a less complex dynamical model than the general problem (in terms of the number of equations and the number of dependent variables), analysis in the circular problem offers further understanding of the motion in a regime that is of increasing interest to space science, as well as new options for mission design. Unfortunately, even with the simplifying assumptions, no general closed form solution to the CR3BP is available. However, particular solutions can be determined. Of notable interest are the equilibrium solutions, which represent locations where the infinitesimal particle remains fixed, relative to a frame of reference that rotates with the primaries.

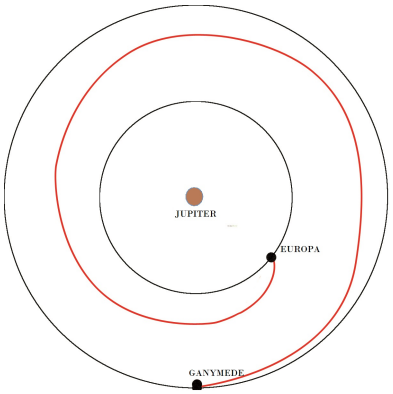

Figure 1.1: Tour of Jovian moons Ganymede and Europa (schematic)

1.1 Literature Review

The N-body problem was first studied by Sir Issac Newton in the 17th century. In 1687, Newton offered significant mathematical insight into the mutual dynamical interactions between multiple bodies in his book Principia Mathematica [1]. However, when more than two bodies are involved, no convenient closed form solution existed. In 1772, Leonhard Euler suggested simplifying assumptions when attempting to explain the motion of the Moon under the influence of the gravity fields of the Earth and the Sun. He introduced the concept of observations from the perspective of a synodic frame. Further exploration of the underlying mathematics associated with this rotating coordinate frame in the Three Body Problem (3BP) shortly led to many new discoveries. In the same year, Joseph Louis Lagrange shared the discovery of five equilibrium points in the synodic frame, where these enable many unique mission applications today. In 1832, Carl Gustav Jacob Jacobi published the observation of an integral of motion in the sidereal frame which was later also reformulated in the synodic frame [3]. This constant established a link between the energy of a spacecraft along its trajectory and the regions of inaccessible space in the CR3BP configuration space, where their boundaries are denoted zero-velocity surfaces (ZVS) [3]. Such structures were employed by George William Hill (1878) in concluding that the Moons range of motion was bounded relative to the Earth. In 1897, Heinrich Bruns proved the non-existence of any other constant of motion in the three-body problem. Two

years later, Jules Henri Poincare also proved the lack of a non-algebraic constant of motion, i.e., the restricted three-body problem problem is non-integrable [3]. Poincare also confirmed the existence of periodic solutions in the restricted three-body problem. In addition to proving that Jacobis constant is the only available integral of the motion in the CR3BP, Poincare (1899) suggested the existence of periodic orbits in the CR3BP system and also introduced the concept that surfaces of sections can offer insight concerning their evolution [4]. Research efforts in the three-body problem slowed for over half a century until Victor G. Szebehely[2] thoroughly detailed the derivation and particular solutions in the restricted three-body problem. Based on the work of Poincare, further developments were accomplished by Birkhoff (1915), Moulton (1920s), Wintner (1941), as well as Kolmogorov and Siegel in the 1950s [5]. As the digital age trickled into the space arena in the 1960s, the pace of progress in this area of research quickened, and its breadth broadened. Today, the CR3BP framework is exploited to design trajectories for impulsive and continuous thrust systems alike, for scenarios ranging from missions to the Moon and beyond.

Recently, mission designs based on the restricted three body problem [6] are of great scientific interest due to low energy consumption. The study about restricted three body problem which has evolved over the past four centuries, has its roots on Newton's law of gravitation .The points of dynamic equilibrium[7] are the solutions of the Eulerian and Lagrangian theories and are named as Lagrangian points or libration points. This area was further explored by Carl Jacobi and George Hill, which resulted in the discovery of Jacobi constant and Hill's regions respectively. It was in 1968 that scientists first exploited the idea of libration Point mission ("Lunar Far -Side Communication Satellites"). Thereafter, several attempts were made including the last launch to SunEarth L_2 in 2013 (Gaia). The focus of the scientific researchers points out the significance of such spatial missions and the an efficient mission design strategy through Lagrange points. The invariant manifold[8][9]structures of the collinear libration points for the spatial restricted three body problem provide the

framework for understanding complex dynamical phenomena from a geometric point of view. The unstable and stable manifolds of the Lagrangian point orbits provide a natural mechanism to transfer natural and artificial bodies in the Solar System. These low energy trajectories ensures significantly better performance than the Hohmann transfer with respect to propellant consumption. Even the trajectories consume zero energy, one of the important features related to periodic trajectories is the instability of motion, which requires the application of station keeping techniques. So far, various techniques have been implemented for trajectory correction maneuver. And the correction maneuvers were attained by merging the invariant manifold dynamics with the low thrust propulsion [5].

There are several major types of low energy orbit planning, each of which focuses on navigating a different area of the solar system. The first type investigates navigating the area near Lagrange points and uses differential equations to describe the manifolds created by the paths of unpropelled particles as they move through the region and are affected by gravity. Lo [14], Koon, Marsden, and Ross have contributed greatly to this area. This type of low energy orbit planning is most closely related to this project as it focuses on the same area of space and utilizes similar orbit shapes. These orbits have been used to navigate near the Earth and then enter interplanetary space. Another type of low energy orbit planning focuses on systems with multiple bodies in resonant orbits. This approach creates a kick function to characterize how much a planetary body will affect another object's orbit depending on how closely they pass each other. Although this works best in the system of Jupiters moons, where orbit periods are relatively small and there are many moons with which to interact, the studies of Grover and Ross [15] reveal principles that are useful when low energy spacecraft initially enter interplanetary space. Their method may be used to adjust the orbit of a spacecraft so that it can reach another planet. The third type of low energy orbit planning focuses on navigating interplanetary space using gravity assist maneuvers with several planets. Studies in this area have achieved fascinating

results, and show that it is possible to navigate the entire solar system through a network of gravity assist maneuvers at different energy levels. Strange and Longuski demonstrate the general principles [16], and Petropoulos, Longuski, and Bonfiglio show how to optimize these gravity assists [7]. Since navigation with gravity assists allows for relatively easy, low energy access to the solar system once a spacecraft can get to another planet, this project focuses on planning the low-energy orbits near Earth and connecting these orbits to the larger interplanetary gravity-assist network.

The approach in [11] is used to design a new mission concept wherein a spacecraft leap-frogs" between moons, orbiting each for a desired duration in a temporary capture orbit. Using a gravitional boost, from Ganymede to go from a joviocentric orbit beyond the orbit of Ganymede to a ballistic capture orbit around Europa. Mission Employs dynamical channels in the phase space (tubes in the energy surface which naturally link the vicinity of Ganymede to the vicinity of Europa). In [12], Lobe dynamics in the restricted three-body problem is used to design orbits with prescribed itineraries with respect to the resonance regions within a Hills region. The application is the design of a low energy trajectory to orbit three of Jupiters moons using the patched three-body approximation (P3BA). Switching region is introduced which is the P3BA analogue to the sphere of influence. In an another work [14], by approximating the dynamics of the Jupiter-Europa-Ganymede-spacecraft 4-body problem as two 3-body sub problems,intersections between the channels of transit orbits enclosed by the stable and unstable manifold tubes of different moons are used to transfer between 2 moons. A low energy transfer trajectory from Ganymede to Europa that ends in a high inclination orbit around Europa was designed. By performing small maneuvers to achieve a particular moon/spacecraft geometry at close approach, the spacecraft can jump between mean motion resonances with the moon.

1.2 Applications of Low-Energy Orbits

There are several instances where spacecraft have utilized low-energy orbits to great effect. The Genesis spacecraft used a series of Earth-Sun L1 and L2 Halo orbits to collect solar wind samples. Another example is the Hiten, a Japanese spacecraft designed to relay signals for the Hagoromo. After the Hagoromo failed, a low-energy transfer to the moon was executed, allowing the Hiten to gain moon orbit even though it had less fuel than was believed to have been needed, making the mission a success. The most famous use of low-energy maneuvers are the gravity assists used by Mariner 10, Pioneer 10 and 11, and Voyager I and II. Low-energy orbits allow spacecraft to navigate in Earths Neighborhood for extended periods of time, requiring only enough fuel to correct for navigation error. One application of these paths currently being discussed could aid in climate engineering and mitigate global warming. Many unmanned spacecraft could be launched using these paths, erecting a deflective sun shield at the Earth-Sun L1 point. Also, Earth- Moon Lagrange points have been suggested as positions where repair crews could gain access to satellites. The possibilities for low-energy paths within the Earths Neighborhood are significant. Another practical use of low-energy orbits would be to aid in the transit of heavy spacecraft, such as unmanned supply crafts or cargo crafts for asteroid mining. Since it requires a large amount of fuel to initially launch heavy spacecraft, there would be little fuel still available in space with which to maneuver, making such a mission a good candidate for low-energy orbits. Since these paths take longer to execute than traditional methods, these supply crafts could be launched ahead of the primary mission and then wait in orbit near the destination. This method would allow larger-scale missions in remote parts of the solar system because of the increased availability of materials. In the case of asteroid mining, low-energy orbits could provide a cost-effective method for transportation across vast distances.

1.3 Problem Definition

A Single Spacecraft is designed to orbit 2 Galilean moons of Jupiter, Ganymede and Europa, using space manifold dynamics. The key ideas is to treat the Jupiter-Ganymede-Europa-spacecraft 4-body problem as two coupled circular restricted 3-body problems, Jupiter-Ganymede-spacecraft and Jupiter-Europa-spacecraft systems and use the stable and unstable manifolds of periodic Lyapunov orbits about the Jupiter-Ganymede Lagrange points to provide a low energy transfer from beyond the orbit of Ganymede to a temporary capture around Ganymede, to the stable manifolds of periodic orbits around the Jupiter- Europa Lagrange points. Then use the stable manifolds of the periodic orbits around the Jupiter-Europa Lagrange points to provide a ballistic capture about Europa.

1.4 Organisation of Thesis

This dissertation is divided into six chapters:

Chapter 2 deals with the fundamental theory involved in dynamics of Three Body Problem. PCRTBP is defined and the equations of motion (relative to a rotating frame) for the spacecraft are analyzed. The equilibrium points (libration points) are identified. The existence of an energy integral(called Jacobi Constant) is utilized for obtaining the Zero Velocity Curves. The allowable region of motion and the unique orbits occurring in PCRTBP are simulated.

In Chapter 3, a periodic orbit around the libration point is generated using differential correction procedure. State transition matrix and monodromy matrix are defined which are used to generate manifolds from periodic orbit. Heteroclinic connection and Homoclinic Trajectories are studied. Different Poincare Sections which are used for end to end transfer are defined.

Chapter 4 presents a zero ΔV trajectory from L_2 to L_1 of Ganymede. Also an algorithm for end to end trajectory from Ganymede to Europa is obtained. ΔV

required for transfer is found.

The system is nonlinear and highly dependent on initial conditions. Chapter 5 deals with design of a non linear controller. Dynamic equations are obtained and a controller based on the dynamic inverse is synthesized for the purpose of stabilization and trajectory tracking.

Chapter 2

Three Body Problem

2.1 Introduction

To get a spacecraft from, Earth to other parts of the solar system (Interplanetary mission) it is necessary to find solutions for the motion of the spacecraft under the influence of N bodies which is a very difficult problem. So we decompose these n-body problem into a number of 3 body problem. This chapter provides a technical foundation about the dynamical structure of 3 body Problem.

2.2 N - Body Problem

The general n body problem (nBP) describes the motion of a body(mi) in a system of n bodies. Under the assumption that there are no external forces other than the gravitational attraction, the force exerted by j^{th} body on i^{th} body is given by the Newton's law of universal gravitation.

$$F_i = \Sigma \frac{G m_i m_j}{|r_{ji}|^3}$$

Since all the bodies are in relative motion the resulting force vector is continuously changing. An analytical solution to the n-body problem is difficult to obtain, so numerical methods are usually employed. Although this equation offered some insight

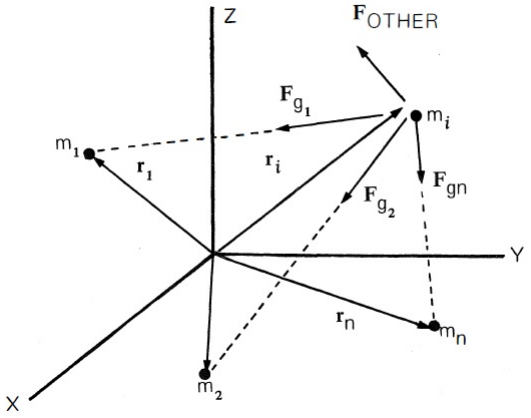

Figure 2.1: n-body problem

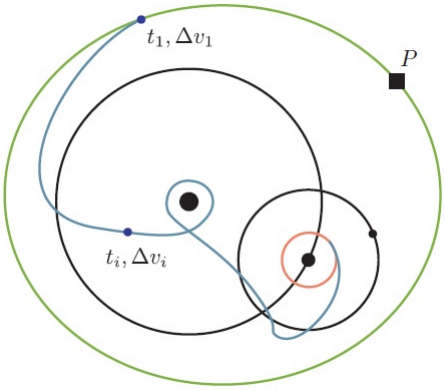

Figure 2.2: A spacecraft P with an impulsive controls in the gravitational field of N massive bodies .

into the dynamical properties of the problem, the information was insufficient to obtain high accuracy numerically integrated solutions. Hence, there was a need for a simplified model and the trajectory designers started to explore the two body problem (2BP),through the patched conic method. The two body problem gives the relative motion of a body about another body. Eg:- Hohmann transfer

Consider the situation shown in Figure 2.2, where we have a spacecraft, approximated as a particle, P, in the gravitational field of N massive bodies. We assume P has a small enough mass that it does not influence the motion of the N massive bodies, which move in prescribed orbits under their mutual gravitational attraction. In the solar system, one can think of a moon, (M_2, in orbit around a planet, (M_1, which is in orbit around the Sun, M0. The goal of trajectory design is to find a transfer

trajectory which takes the spacecraft from a prescribed initial orbit to a prescribed final orbit using controls. To effect this transfer, we could use high thrust or low thrust propulsion systems. In the low thrust case, we have a small continuous control which can operate at all times. In the high thrust case, we assume that the control is discretized into several instantaneous changes in the spacecraft's velocity ΔV.

$$\Delta \mathrm{V} = -\mathrm{V}_e \frac{\Delta m}{m}$$

where m is the mass of the rocket and Δm is the mass of propellant ejected at an exhaust velocity V_e

As spacecraft are limited in the amount of fuel that they can carry on board for their journey, we often want to consider an optimal control problem: minimize the fuel consumed. It is typical in space missions to use the magnitude of the required ΔV as a measure of the spacecraft fuel performance. The propellant mass is a much less stable quantity as a measure of spacecraft performance, since it is dependent on the spacecraft mass and various other parameters which change frequently as the spacecraft is being built. The ΔV comes from astrodynamics considerations only and is independent of the mass and type of spacecraft. Thus, for a given mission objective, one generally wants to minimize ΔV. For missions that utilizes Hohmann transfer, the speed of the spacecraft relative to the bodies is high and therefore the time during which the acceleration on the spacecraft due to two bodies is comparable is very short, and results in a minor perturbation away from a conic solution. But when one needs to deal with the unpropelled, or ballistic, capture regime of motion,where the relative speed is low, a three-body decomposition of the solar system is necessary.

2.3 Three Body Dynamics

In the general three body problem, there are three massive bodies moving under their mutual gravity interactions and the interest is to study the motion of all the three bodies based on Newton's law of gravitation. To begin with, we restrict the motion of all the bodies to a common plane, so the phase space is only four-dimensional. As in the patched conic approach, the patched three-body approach uses solutions obtained from two three-body problems as an initial guess for a numerical procedure called differential correction which converges to a full four-body solution. As an example of such a problem where there is no control, consider the four-body problem where two adjacent giant planets compete for control of the same comet (e.g., Sun-Jupiter-comet and Sun-Saturn-comet). When close to one of the planets, the comet's motion is dominated by the corresponding planet's perturbation. Between the two planets, the comet's motion is mostly heliocentric and Keplerian, but is precariously poised between two competing three-body dynamics, leading to complicated transfer dynamics between the two adjacent planets. When we consider a spacecraft with control instead of a comet, we can intelligently exploit the transfer dynamics to construct low energy trajectories with prescribed behaviors, such as transfers between adjacent moons in the Jovian system. However, it was not possible to obtain a closed -form solution. Thus, to reduce the analytical complexity, further simplifications were introduced into the system which resulted in the restricted three body problem.

2.4 PCRTBP

The Restricted Problem of Three Bodies[9] is concerned with the motion of an infinitesimally lighter mass (m) in a binary system of heavy masses M_1 and M_2 ($M_1 > M_2$) rotating about their centre of mass. In order to reach a solution, the following assumptions are made.

1. All the three bodies move in the same plane.

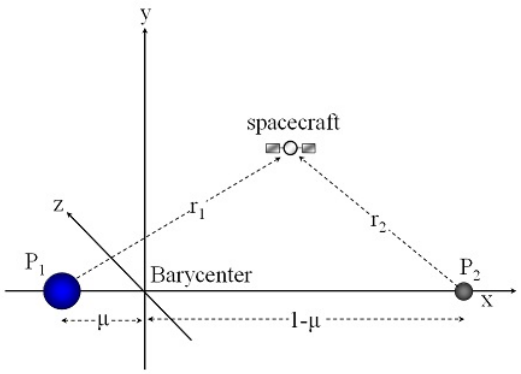

Figure 2.3: Restricted three body problem

2. The heavy bodies travel in circular orbits.

3. The secondary body (m) has negligible effect on the primaries (M_1 and M_2)

To investigate this problem, consider the system in a reference frame (x, y) which is rotating with respect to an inertial frame (fixed frame). The rotating frame (synodic frame) shares the same origin as that of the inertial frame (X,Y) which is the centre of masses and it rotates at the same speed as the binary system composed of the primaries

The coordinate system is such that the x axis is defined along the line that goes from the earth to the moon. The z axis is aligned in the same direction as that of the angular velocity vector of the primaries and the y axis is the one perpendicular to both the x z axis. The need for this rotating reference frame is that, if the system is examined in an inertial frame it is difficult to understand the motion of the massive bodies since the coordinates of both M_1 and M_2 are time dependent. But in a synodic frame, the primaries remain fixed while the third body (e.g: a satellite or all asteroid) rotates about them. For obtaining the dimensionless values, the units are scaled as follows:

- The unit of mass is taken to be the sum of masses of primary and secondary(M_1 + M_2) = 1 Mass Unit (MU)

- The unit of length is chosen to be the constant separation between M_1 and M_2 = 1 Distance Unit (DU)

- The unit of time is chosen such that the orbital period of M_1 and M_2 about their centre of mass is $2\Pi = 1$ Time Unit(TU)

which makes both the gravitational constant G and angular velocity ω of the system to be unity. The normalized units is used for all the discussions in this report. When appropriate, these are converted to dimensional units (e.g., km, km/s, seconds) to scale a problem. This will be particularly important during decomposing of a N-body problem into several 3-body sub problems. The conversion from units of distance, velocity, and time in the unprimed, normalized system to the primed, dimensionalized system is

- distance d'= Ld,
- velocity s'= V s,
- time t'= $\frac{T}{2\Pi}t$

where L is the distance between the centres of $M_1$and M_2, V is the orbital velocity of M_1, T is the orbital period of M_1 and M_2. The only parameter of the system is the mass parameter.

$$\mu = \frac{M2}{M1 + M2}$$

The orbital planes of Ganymede and Europa are within 3 degree of each other, and their orbital eccentricities are 0.0006 and 0.0101, respectively. If we restrict the motion of the spacecraft to their approximately common orbital plane, then the coupled PCR3BP is an excellent starting model for illuminating the transfer dynamics between these moons. Recalling the equations for the PCR3BP, the two main bodies, have a total mass that is normalized to one. Their masses are denoted, as usual, by $m_J = 1 - \mu$ and $m_M = \mu$ respectively. These bodies rotate in the plane counterclockwise about their common centre of mass and with the angular velocity normalized to one. The third body, which we call the spacecraft, has mass zero and

is free to move in the plane. The mass parameters for different systems are given in table2.1

System	μ	L	V	T
Sun-Jupiter	$9.537\text{x}10^{-4}$	$7.784\text{x}10^{8}$	13.102	$3.733\text{x}10^{8}$
Jupiter-Ganymede	$7.804\text{x}10^{-5}$	$1.070\text{x}10^{6}$	10.909	$6.165\text{x}10^{5}$
Jupiter-Europa	$2.528\text{x}10^{-5}$	$6.711\text{x}10^{5}$	13.780	$3.060\text{x}10^{5}$
Jupiter-Callisto	$5.667\text{x}10^{-5}$	$1.833\text{x}10^{6}$	8.266	$1.438\text{x}10^{6}$
Jupiter-Lo	$4.704\text{x}10^{-4}$	$4.218\text{x}10^{5}$	17.390	$1.524\text{x}10^{5}$

Table 2.1: Table of (M_1-(M_2 systems in the solar system.

2.5 Coordinate Transformation

Let X-Y-Z be an inertial frame with origin at the (M_1-M_2 centre of mass, as in Figure 2.4, where the X-Y plane is the orbital plane of the primaries. Consider the set of axes x and y depicted in Figure 2.4. The x-axis lies along the line from M_1 to M_2 with the y-axis perpendicular to it, completing a right-handed coordinate system. The x-y frame rotates with respect to the X-Y inertial frame with an angular velocity equal to the mean motion, n, of either mass (unity in the normalized units). This coordinate frame is referred as the rotating frame or the M_1-M_2 rotating frame. Assume that the two frames coincide at $t = 0$. Let (X,Y,Z) and (x,y,z) be the position of P in the inertial and rotating frames, respectively. In normalized units, we have the following transformation of the particle's position between the two frames:

$$\begin{bmatrix} X \\ Y \\ Z \end{bmatrix} = A_t \times \begin{bmatrix} x \\ y \\ z \end{bmatrix}$$

where

$$A_t = \begin{bmatrix} cost & -sint & 0 \\ sint & cost & 0 \\ 0 & 0t & 1 \end{bmatrix}$$

Differentiating gives us the transformation of velocity components from the rotating to the inertial frame.

$$\begin{bmatrix} X \\ Y \\ Z \end{bmatrix} = \dot{A}_t \times \begin{bmatrix} x \\ y \\ z \end{bmatrix} + A_t \times \begin{bmatrix} \dot{x} \\ \dot{y} \\ \dot{z} \end{bmatrix}$$

$$\begin{aligned} \begin{bmatrix} X \\ Y \\ Z \end{bmatrix} &= \dot{A}_t \times \begin{bmatrix} x \\ y \\ z \end{bmatrix} + A_t \times \begin{bmatrix} \dot{x} \\ \dot{y} \\ \dot{z} \end{bmatrix} \\ &= -A_t \times J \times \begin{bmatrix} x \\ y \\ z \end{bmatrix} + A_t \times \begin{bmatrix} \dot{x} \\ \dot{y} \\ \dot{z} \end{bmatrix} \\ &= -A_t \times \begin{bmatrix} \dot{x} - y \\ \dot{y} + x \\ \dot{z} \end{bmatrix} \end{aligned}$$

where

$$J = \begin{bmatrix} 0 & 1 & 0 \\ -1 & 0 & 0 \\ 0 & 0 & 0 \end{bmatrix}$$

2.6 Equations of Motion.

The equations of motion could be derived using a little elementary mechanics as follows. Considering rotating frame discussed in section 2.4, distance between the primaries is unity and they rotate with unit angular velocity. The two bodies are located on the x axis at the points $(-\mu, 0)$ and $(1-\mu, 0)$. Let the position of the

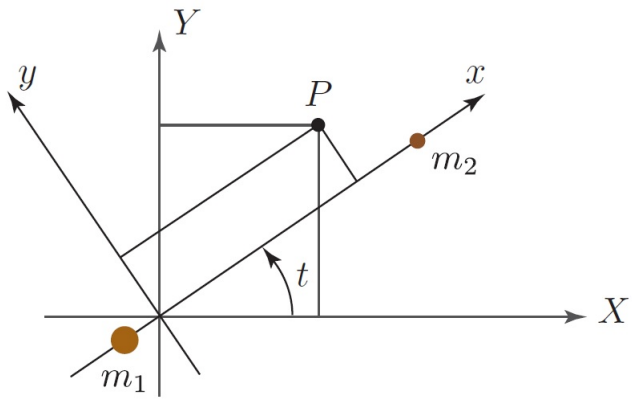

Figure 2.4: Inertial and rotating frames.

third body be denoted (x, y) in the rotating frame. The kinetic energy of this third body in a frame rotating with unit angular velocity is the usual $\frac{1}{2}mv^2$ expression

$$K(x, y, \dot{x}, \dot{y}) = \frac{1}{2}[(\dot{x} - y)^2 + (\dot{y} + x)^2] \tag{2.1}$$

Let r_1 be the distance from the third body to the first primary and r_2 be the distance to the second primary,

$$r_1 = \sqrt{(x + \mu)^2 + y^2 + z^2} \tag{2.2}$$

$$r_2 = \sqrt{(x - 1 + \mu)^2 + y^2 + z^2} \tag{2.3}$$

Then the gravitational potential energy of the third body is, again in normalized units,

$$U(x, y) = -\frac{1 - \mu}{r_1} - \frac{\mu}{r_2} \tag{2.4}$$

The Lagrangian of the third body is its kinetic minus potential energies given by

$$L(x, y, \dot{x}, \dot{y}) = K(x, y, \dot{x}, \dot{y}) - U(x, y) \tag{2.5}$$

The equations of motion is obtained by writing down the corresponding Euler

Lagrange equations given by

$$\frac{\partial L}{\partial q^i} - \frac{d}{dt}\frac{\partial L}{\partial \dot{q}^i} = 0$$

Therefore equations of motion can be written as

$$\ddot{x} - 2\dot{y} = \frac{\partial \bar{U}}{\partial x} \tag{2.6}$$

$$\ddot{y} + 2\dot{x} = \frac{\partial \bar{U}}{\partial y} \tag{2.7}$$

where the effective potential is

$$\bar{U} = U - \frac{x^2 + y^2}{2} \tag{2.8}$$

Thus the equations of motion of the spacecraft can be summarized as

$$\ddot{x} = \Omega_x + 2\dot{y} \tag{2.9}$$

$$\ddot{y} = \Omega_y - 2\dot{x} \tag{2.10}$$

$$\Omega = -\bar{U}$$

Therefore

$$\ddot{x} = x + 2\dot{y} - \frac{(1-\mu)}{r_1^3}(x+\mu) - \frac{\mu}{r_2^3}(x-(1-\mu)) \tag{2.11}$$

$$\ddot{y} = y - 2\dot{x} - \frac{(1-\mu)}{r_1^3}y - \frac{\mu}{r_2^3}y \tag{2.12}$$

$$\ddot{z} = \frac{(1-\mu)}{r_1^3}z - \frac{\mu}{r_2^3}z \tag{2.13}$$

Notice that both the Lagrangian form of the equations in rotating coordinates give a time-independent system. Viewed as a dynamical system, it is a dynamical system in a 4-dimensional phase space, viewed as (x,y,$\dot{x}$,$\dot{y}$)space, subsets of R^4 which exclude the singularities at the positions of the primaries.

2.7 Libration points

Equilibrium occurs when the third body moves in a circular orbit with the same frequency as the primaries, so that it is stationary in the rotating frame. The PCRTBP consists of equilibrium points where the net centripetal force required for the movement of a lighter body is provided by the gravitational field of the primaries. We find these points by finding the equilibrium points, in the standard sense of ODE's, of the equations (2.1). This task is equivalent to finding the critical points of the effective potential. There are five such points. Three collinear points on the x axis that were discovered by Euler around 1750 and are denoted L_1, L_2, L_3 and there are two equilateral points discovered by Lagrange around 1760 and are denoted L_4 and L_5. They are indicated in Figure 2.5. Equations (2.1) may be interpreted as those of a particle moving in an effective potential plus a magnetic field. The graph of the effective potential is shown in Figure 2.6. This figure also shows the region one gets by imposing conservation of energy and the simple inequality that the kinetic energy is positive. Thus, at a given energy level E, the third body can only move in the region given by the inequality $E - \Omega \geq 0$. This is called the Hill's region which is discussed in detail, later in this chapter. It is obtained by intersecting the graph of the effective potential with a horizontal plane.

For analyzing the stability of a libration point, the PCR3BP equations of motion are linearized around that point. It is differential of the vector field that provides the linear flow dynamics near the equilibrium point.The linear behaviour at these points are of the type "saddle x centre". That is, the motion near the vicinity of these libration points has trajectories which stays bound to the equilibrium point (centre) and those with hyperbolic behaviour(saddle). Hence, the equilibrium positions $L_1, L_2, L_3$are unstable with real eigen values and for any libration orbit about the unstable points additional station keeping control is required.The famous Lyapunov theorem says that there is a family of periodic orbits surrounding each of these points; one can think of this as meaning that one can go into orbit about these points. These

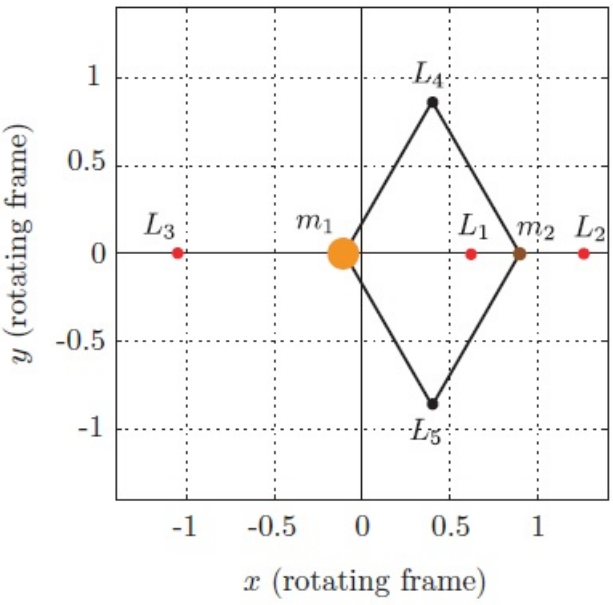

Figure 2.5: Libration Points

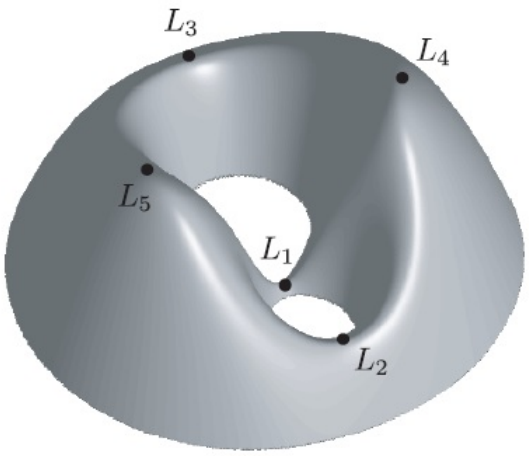

Figure 2.6: The graph of the effective potential in the 3-body problem

planar periodic orbits are called **Lyapunov orbits**, while their counterparts in the 3D problem are called **halo and Lissajous orbits**.The stability of the triangular configuration has "centre x centre" behaviour. Thus, the last two equilibrium positions are stable with complex conjugate eigen values. So, the motion of a spacecraft around L_4 and L_5 remains within that neighbourhood itself.

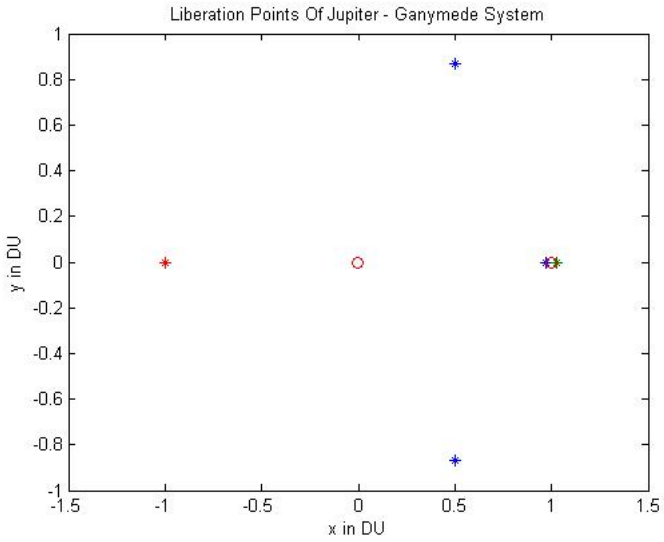

Figure 2.7: Simulation of Liberation Points

2.8 Jacobi Constant and Energy Integral

Since the equations of motion of the CR3BP (2.11) is independent of time, they have an energy integral of motion. Physically, the measurement of the particle's position and velocity in either the inertial or rotating frames determines the value of the energy associated with the particle's motion. With a particular velocity, there exists an upper bound for the energy of a body. Thus, for the above equations of motion there exists an energy integral called Jacobi Integral (C) which at zero velocity partitions the configuration space into bounded and unbounded regions of motion (Hill's curve).There are no other integrals constraining the motion of the particle, making the PCR3BP a non-integrable problem.

The Energy and Jacobi integral is related by $C = -2E$. Energy is given by

$$E(x, y, \dot{x}, \dot{y}, \dot{z}) = \frac{1}{2}[(\dot{x}^2 + \dot{y}^2 + \dot{z})^2 + \bar{U}(x, y, z)] \tag{2.14}$$

Jacobi Integral is given by

$$C(x, y, z, \dot{x}, \dot{y}, \dot{z}) = -[(\dot{x}^2 + \dot{y}^2 + \dot{z})^2 - 2\bar{U}] \tag{2.15}$$

The existence of the Jacobi integral is derived directly from the equations of motion.

$$\frac{d}{dt}(\dot{x}^2+\dot{y}^2+\dot{z})^2 = 2(\dot{x}\ddot{x}+\dot{y}\ddot{y}+\dot{z}\ddot{z}) = 2[\dot{x}(2\dot{y}-\bar{U}_x)+\dot{y}(-2\dot{x}-\bar{U}_y)+\dot{z}(-\bar{U}_z) = 2\frac{d}{dt}(-U)$$

Therefore

$$\frac{d}{dt}C = \frac{d}{dt}[-(\dot{x}^2+\dot{y}^2+\dot{z})^2 - 2\bar{U}] = 0 \tag{2.16}$$

In simplified form,Jacobi Integral could be written as

$$C = (x^2+y^2) + 2\frac{(1-\mu)}{r_1} + 2\frac{\mu}{r_2} - (\dot{x}^2+\dot{y}^2) \tag{2.17}$$

and the total energy

$$E = \frac{1}{2}(\dot{x}^2+\dot{y}^2) - \frac{1}{2}(x^2+y^2) - \frac{(1-\mu)}{r_1} - \frac{\mu}{r_2} \tag{2.18}$$

Libration point	**x-coordinate**	**y-cordinate**	**Jacobi Constant**
L_1	0.970589422811690	0	3.007640671432188
L_2	1.029839658372774	0	3.007536637327930
L_3	-1.000032508333309	0	3.000078019873091
L_4	0.499921980000000	0.866025403784439	2.999921986087121
L_5	0.499921980000000	-0.866025403784439	2.999921986087121

Table 2.2: Liberation Points and Jacobi Constant of Jupiter Ganymede System

2.9 Hill's Regions.

The energy manifold M or energy surface is given by setting the energy integral equal to a constant e.For a fixed μ and energy e,the surface M will be a three-dimensional surface embedded in the four-dimensional phase space. The projections of the energy surface onto the position velocity space yields the region where the motion of the

Libration point	x-coordinate	y-cordinate	Jacobi Constant
L_1	0.979777442431547	0	3.003638024032710
L_2	1.020447783124820	0	3.003604382770088
L_3	-1.000010512500000	0	3.000025229986735
L_4	0.499974770000000	0.866025403784439	2.999974770636553
L_5	0.499974770000000	-0.866025403784439	2.999974770636553

Table 2.3: Liberation Points and Jacobi Constant of Jupiter Europa System

spacecraft is bounded called the Hill's region.The boundary of Hill's Curve is known as the zero velocity curve, and plays an important role in placing bounds on the motion of the particle.

2.9.1 Zero Velocity Curves

The zero velocity curves are the locus of points in the x-y plane where the kinetic energy, and hence the velocity.$v = 0$. The particle is only able to move on the side of this curve for which the kinetic energy is positive. The other side of the curve, where the kinetic energy is negative and motion is not possible, is known as the forbidden realm.It is the zero velocity curve that defines the boundary of the Hill's region. This boundary differentiates the region of position space into Hill's region and forbidden region (where the motion of spacecraft is not possible). The geometry of the Hill's curve changes with value of Jacobi constant.The area outside the Hill's curve indicates the exterior forbidden region whereas the one between the Hill's curves is the interior forbidden region.

2.9.2 The Five Cases of the Hill's Region

For a given μ there are five basic configurations for the Hill's region, corresponding to five intervals of Jacobi Constant value C. We refer to these basic configurations as energy cases.

- **Case 1** , $E < E_1$ or $C > C_1$: If the energy of the particle is below E_1, the

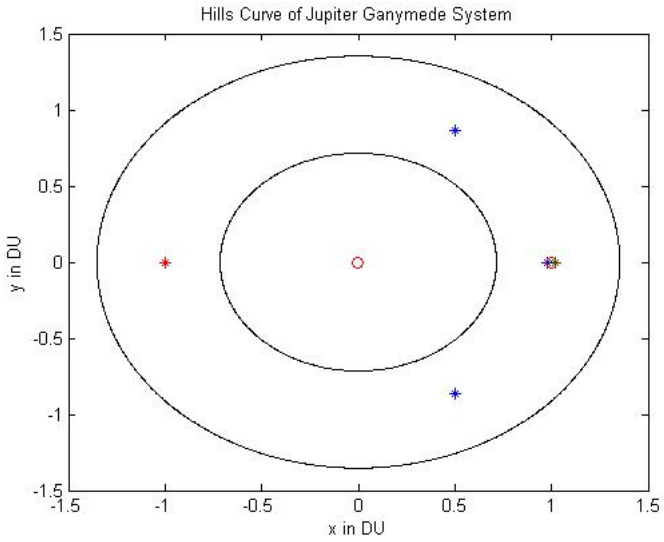

Figure 2.8: Zero Velocity Curve for C>C1

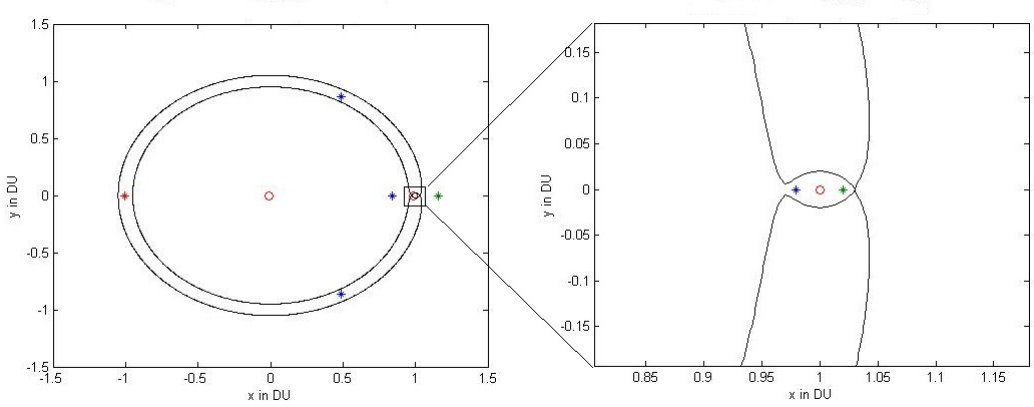

Figure 2.9: Zero Velocity Curve for C1>C>C2

particle cannot move between the realms around M_1 and M_2.

- **Case 2** , $E_1 < E < E_2$ or$C_1 > C > C_2$: If the energy is just aboveE_1, a neck between the realms around M_1 and M_2 opens up, permitting the particle to move between the two realms. The L_1 point is in this neck. The transport between the two adjacent realms is controlled by invariant manifold structures associated to L_1. The particle is still barred from moving between these two realms and the exterior realm extending to infinity.

- **Case 3** , $E_2 < E < E_3$ or$C_2 > C > C_3$: This is the case that concerns us the most that is when the energy is just above E_2. The particle can move between

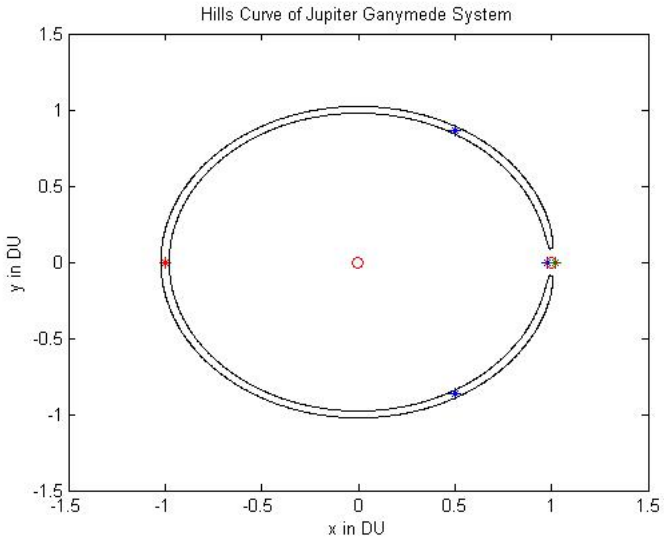

Figure 2.10: Zero Velocity Curve for C2>C>C3

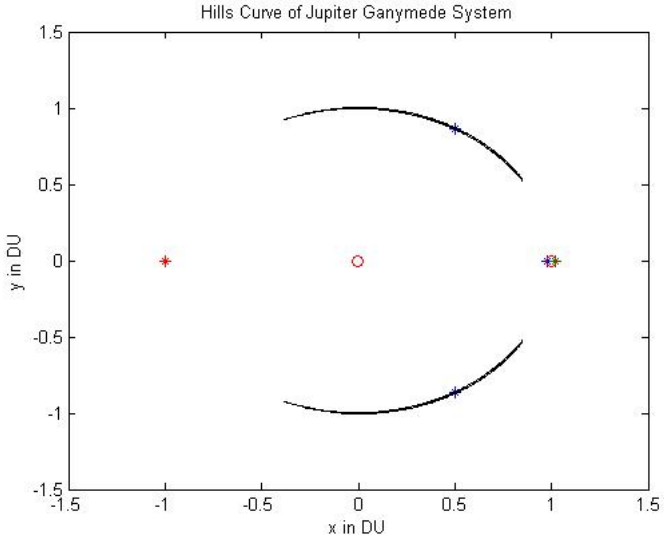

Figure 2.11: Zero Velocity Curve for C3>C>C4

the vicinity of M_1 and M_2 and the exterior realm via a neck around L_2

- **Case 4** ,$E_3 < E < E_4 = E_5$ or$C_3 > C > C_4 = C_5$: In this case the energy is above E_3 but below that of E_4 and E_5.The particle can pass directly from the vicinity of M_1 to the exterior realm via a neck around L_3.

- **Case 5** ,$E > E_4 = E_5$ or$C < C_4 = C_5$: If the energy is aboveE_4 or E_5 the forbidden realm disappears. This is the case where the particle is free to move in the entire x-y plane.

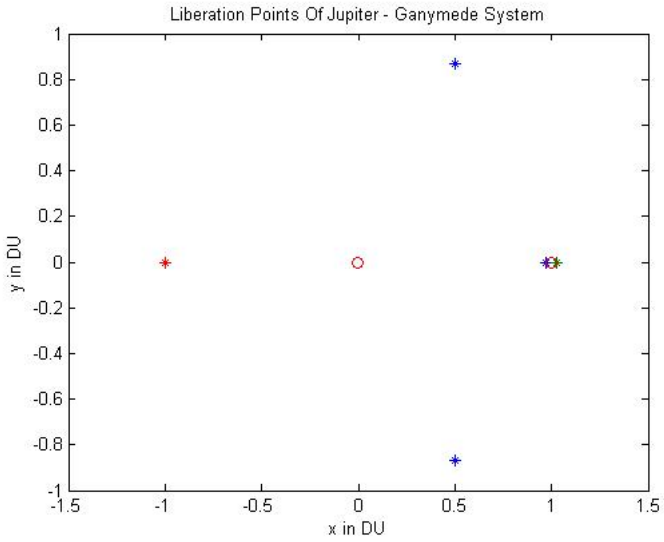

Figure 2.12: Zero Velocity Curve for C<C4

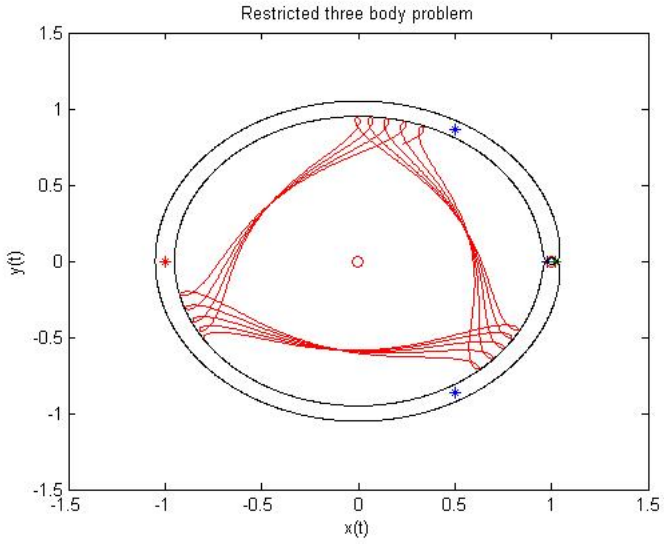

Figure 2.13: Motion of spacecraft for $C > C_1$

From fig 2.13 it is clear that for an initial condition with $C > C_1$ trajectory does not cross Hill's curve

2.10 Mass Parameter μ

The Gravitational parameter or Mass parameter is given by

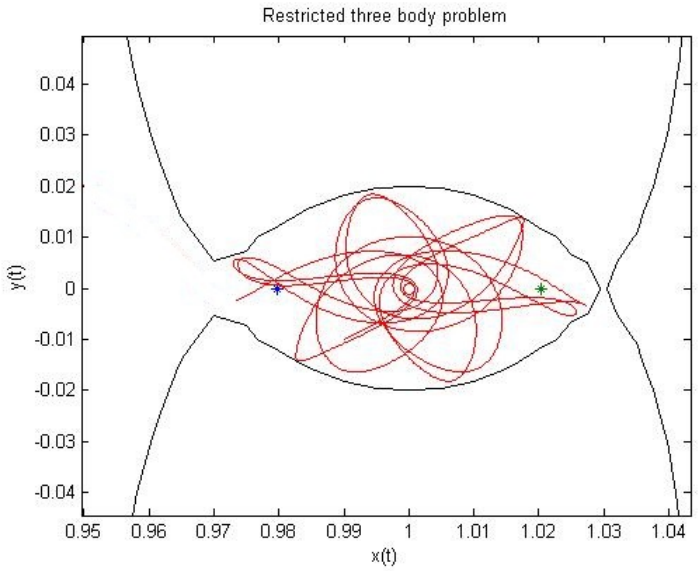

Figure 2.14: Motion of spacecraft for $C_1 > C > C_2$

Sl	System	μ	L_1	L_2	C_1	C_5
a	Pluto-Charon	$1.0967\text{x}10^{-1}$	0.59084	1.26286	3.62349	2.90233
b	Earth-Moon	$1.215\text{x}10^{-2}$	0.83691	1.15567	3.18833	2.98799
c	Sun-Jupiter	$9.537\text{x}10^{-4}$	0.93236	1.06882	3.03875	2.99904
d	Saturn-Titan	$2.366\text{x}10^{-4}$	0.95749	1.04325	3.01576	2.99976
e	Neptune-Triton	$2.089\text{x}10^{-4}$	0.95922	1.04149	3.01453	2.99979
f	Jupiter-Ganymede	$7.804\text{x}10^{-5}$	0.97058	1.02983	3.00764	2.99992
g	Jupiter-Callisto	$5.667\text{x}10^{-5}$	0.97354	1.02681	3.00619	2.99994
h	Jupiter-Lo	$4.704\text{x}10^{-5}$	0.97513	1.02518	3.00548	2.99995
i	Jupiter-Europa	$2.528\text{x}10^{-5}$	0.97977	1.02044	3.00363	2.99997
j	Sun-Earth+Moon	$3.036\text{x}10^{-6}$	0.98999	1.01007	3.00089	2.99999
k	Saturn-Mimas	$6.723\text{x}10^{-8}$	0.99718	1.00282	3.00007	2.99999
l	Mars-Phobos	$1.667\text{x}10^{-8}$	0.99822	1.00177	3.00002	2.99999

Table 2.4: The Liberation Points and Jacobi Constant of Different Systems

$$\mu = \frac{M_2}{M_1 + M_2}$$

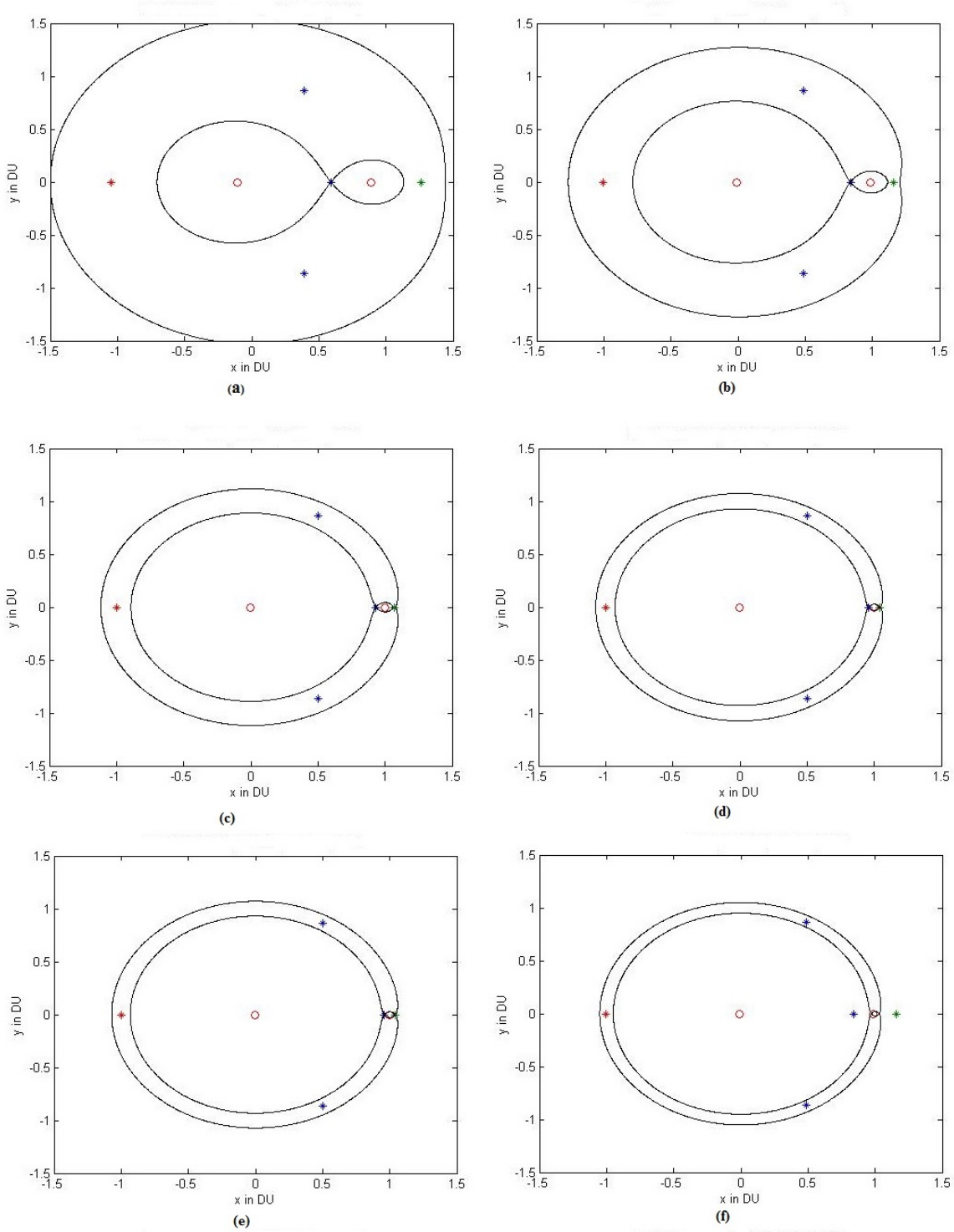

Figure 2.15: Zero Velocity Curve for C=C1 for different systems given in table

The phase space of system is highly dependent on μ. As the value of μ is larger, following observations are obtained:

- The L_1 and L_2 points move away from M_2.

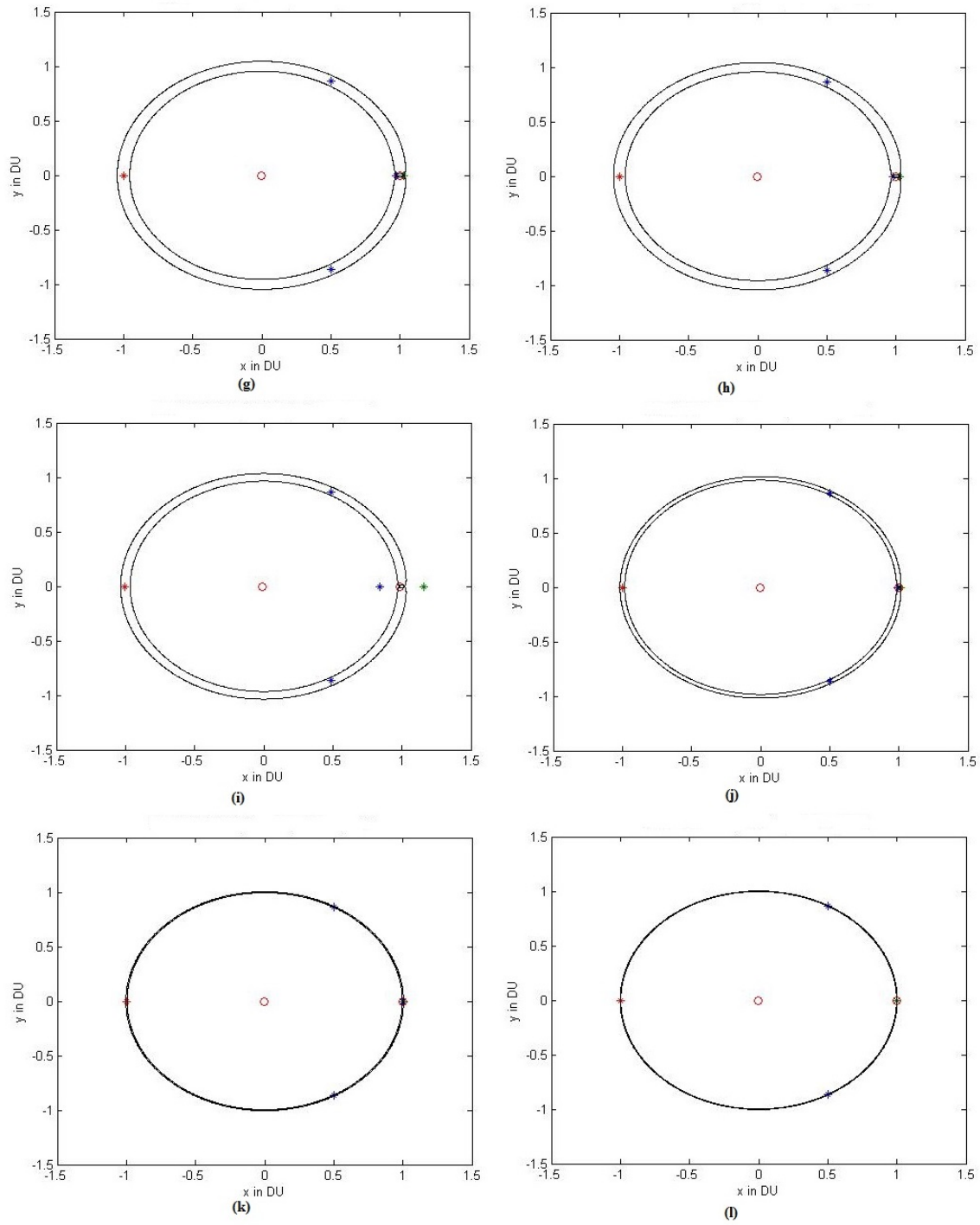

Figure 2.16: Zero Velocity Curve for C=C1 for different systems given in table

- The value of Jacobi Constants increase. Also the range of Jacobi Constant values $[C_1 C_5]$ will be larger.
- The thickness of forbidden region in Hill's curve will be more.

- The 'net like' manifolds are clearly visible.

The observations are tabulated in table 2.4.

2.11 Conclusion

In this chapter some basic terminology for the restricted three body problem was developed and the local dynamics near equilibrium points and their stability are described. .The study revealed that there are three unstable and two stable libration points.Mass parameter and its influence on Libration points and Hill's curve were obtained. An investigation about the regions of motion resulted in different types orbits in PCRTBP stated in the next chapter. The next chapter deals with development of a manifolds.

Chapter 3

Invariant Manifolds

3.1 Introduction

In the 3 body problem, a key role is played by the invariant manifolds of these periodic orbits. Also there exists a network of homoclinic and heteroclinic orbits connecting these periodic orbits[12,15].The invariant manifold structures of L_1 and L_2 provide the framework for understanding and categorizing the motions of spacecraft. Moreover, the stable and unstable invariant manifold tubes associated to periodic orbits around L_1 and L_2 transport material between different realms in a single three body system as well as between primary bodies for separate three-body systems. These tubes can be used to construct new spacecraft trajectories.

3.2 Types of Orbits

In each equilibrium region around L_1 or L_2, there exist four types of orbits as shown in Figure 4.1

1. The periodic or **Lyapunov orbit**.

2. The cylindrical sets of **Asymptotic orbits** that wind onto this periodic orbit (pieces of the periodic orbit's stable and unstable invariant manifold).

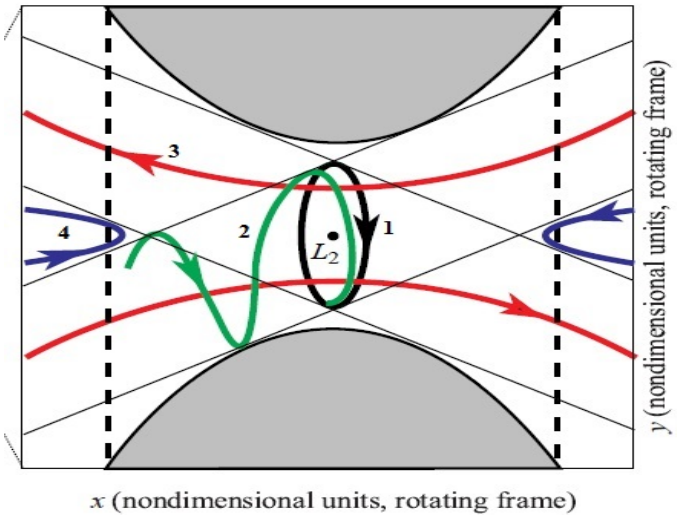

Figure 3.1: Types of Trajectories

3. The **Transit orbits** that the spacecraft uses to make a transit from one region to the other.

4. The **Non-transit orbits** where the spacecraft comes out of one region and pass near the equilibrium point only to fall back into the same region.

3.3 Periodic Orbit or Liapunov Orbit

From the study about the different trajectories in PCRTBP, it can observed the orbits are highly sensitive to the initial conditions i.e., a small change in initial condition results in a completely different trajectory. Construction of Periodic Orbit around L_1 is achieved by following algorithm given below.

Periodic orbit generation using Newton-Raphson (NR) algorithm[11] gives a good approximation of an orbit. The initial trajectory is differentially corrected to obtain a periodic orbit. Each iteration develops a better initial value which in turn results in a more accurate trajectory. For a given initial condition,near L_1, integrate equations of motion forward. Since the Lyapunov orbit is symmetric with respect to the xz-plane, this meets the x-axis twice orthogonally. This is taken as the termination criteria (y=0) for the integration of the equation of motion. If the error condition

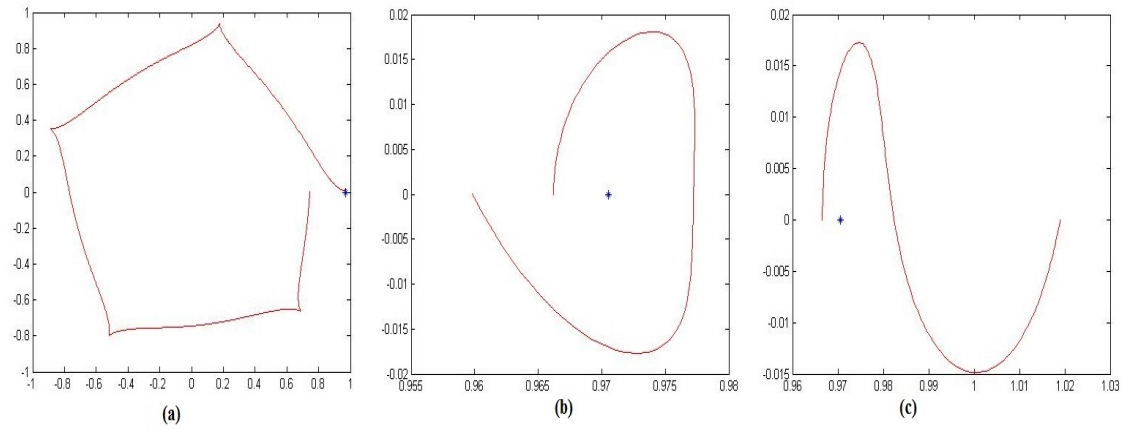

Figure 3.2: Periodic Orbit Generation around L_1

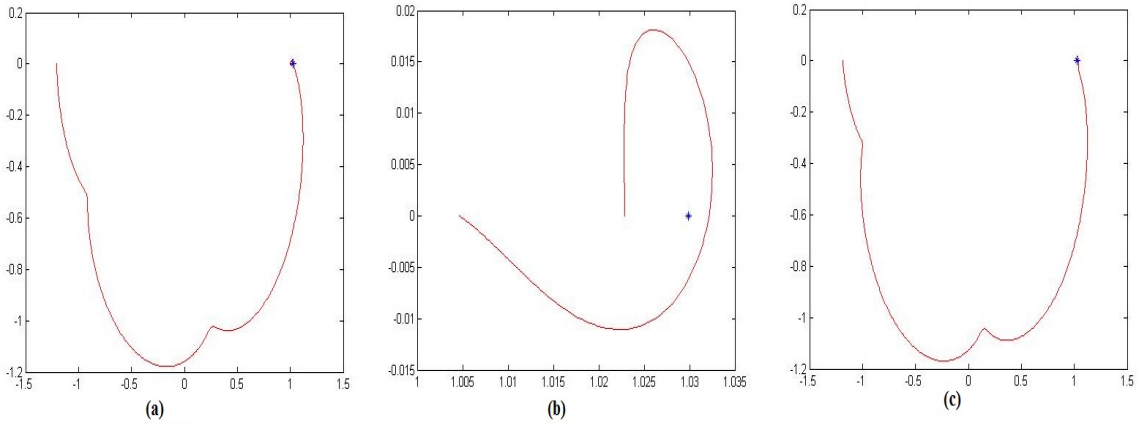

Figure 3.3: Periodic Orbit Generation around L_2

is satisfied, the iterative procedure is stopped or the initial value is perturbed and the procedure is repeated. Here, the error indicates the difference between the final and initial values of position and velocity. Periodic Orbits can be utilized for the generation of manifolds. Thus, it is this closed path that acts as a reference orbit for the generation of stable and unstable manifolds.

3.3.1 Algorithm for Generation of Periodic Orbit

1. Choose a Jacobi Constant value and take an initial x position close to left of libration point L_1.

2. The y and $\dot{x}$ are chosen as zero. The $\dot{y}$ is found from Jacobi integral equation.

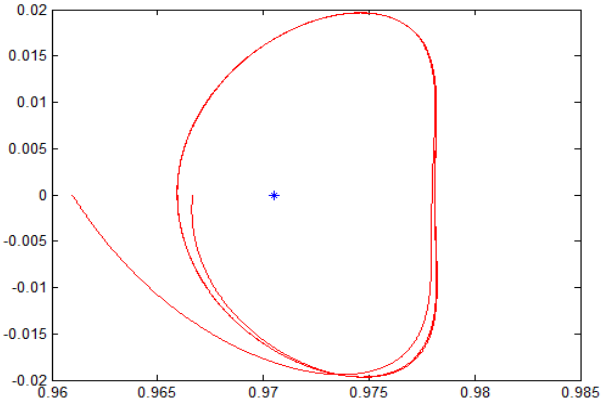

Figure 3.4: Periodic orbit generation using differential correction

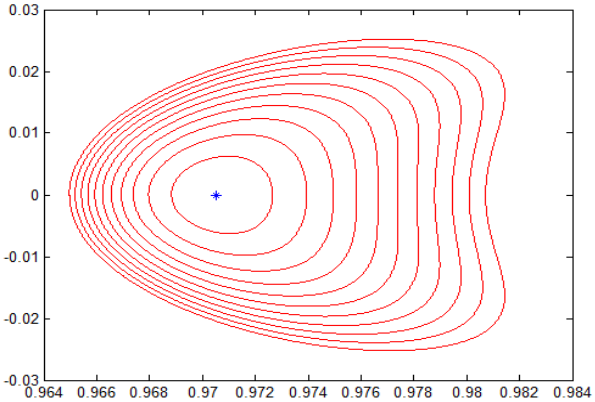

Figure 3.5: Periodic Orbit for different C

This yields any one of trajectory as shown in fig 3.2.

3. If a trajectory similar to (b) is obtained, an iteration strategy is used and trajectory is differentially corrected to obtain a closed periodic (Lyapunov) orbit.

4. If a trajectory similar to (a) is obtained, a very small increase in x position results in (b) and vice verse in case of (c).

Taking an initial x position far from L_1 can produce trajectories other than those shown in fig 3.2. Once an initial x position is obtained for a C value, an iterative procedure is followed, where value of C is slightly varied to C_1 and x obtained after

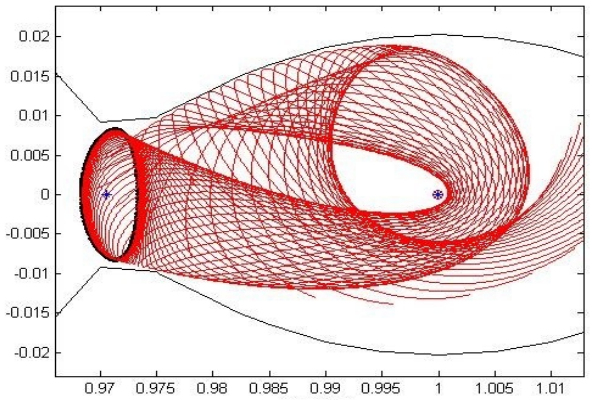

Figure 3.6: L_1 Right Unstable Manifold

differential correction procedure is used to obtain new initial x_1 position for current C_1. Fig 3.4 shows periodic orbits generated for different C using above algorithm.

3.4 Manifolds

The solution surface formed by low -energy trajectories either converging towards (stable) or diverging away (unstable) from a nominal orbit is called a manifold. It the mapping of perturbed state (for a period T) along the direction of stable and unstable eigen vectors of the monodromy matrix which constitutes the stable and unstable manifolds. A spacecraft perturbed along the stable manifold will approach the periodic orbit eventually as $t \to \infty$. whereas the one perturbed along the unstable manifold will exponentially depart the periodic orbit as $t \to \infty$.

First a Liapunov Orbit is generated sround a Libration Point. A set of equidistant points where considered along the periodic orbit by parametrisation of orbit.Each point serves as an initial condition for the forward integration of equation of motion to obtain unstable manifold and backward integration of equation of motion to obtain stable manifold. The right unstable manifold is obtained by perturbing the initial condition along the direction of the unstable eigen vector. .Depending upon the type of perturbation, there are two types of branches for both stable and unstable manifolds. If positive perturbation to x -component is provided to the initial state

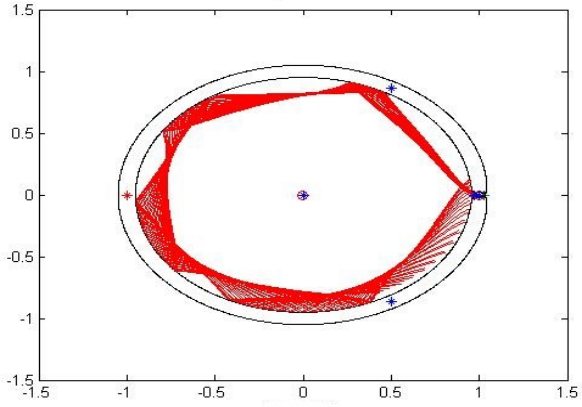

Figure 3.7: L_1 Left Unstable Manifold

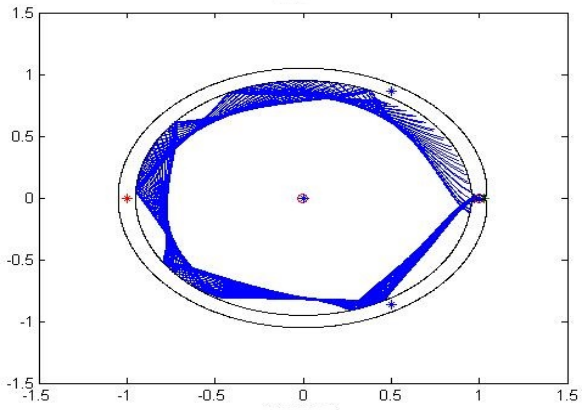

Figure 3.8: L_1 Left Stable Manifold

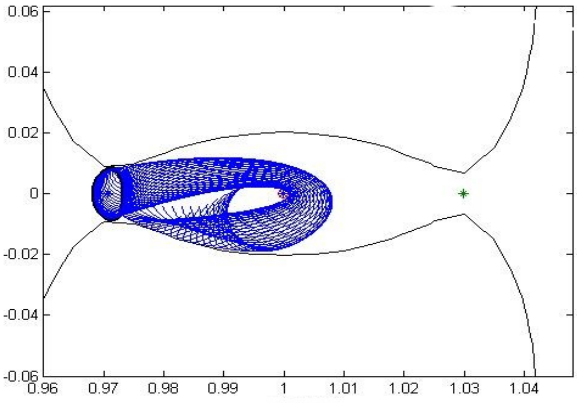

Figure 3.9: L_1 Right Stable Manifold

that results in right branch of manifold, whereas negative perturbation yields the right branch. Thus, the solution space consists of four types of trajectories.

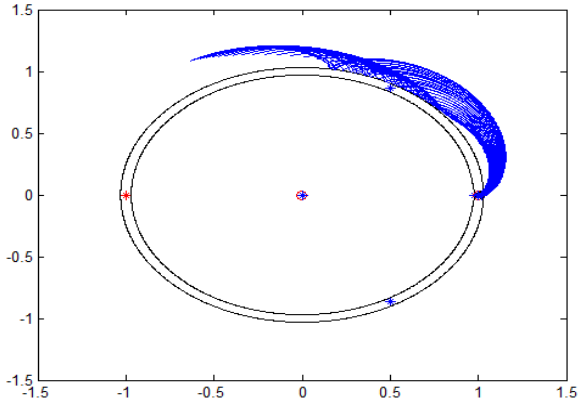

Figure 3.10: L_2 Right Stable Manifold

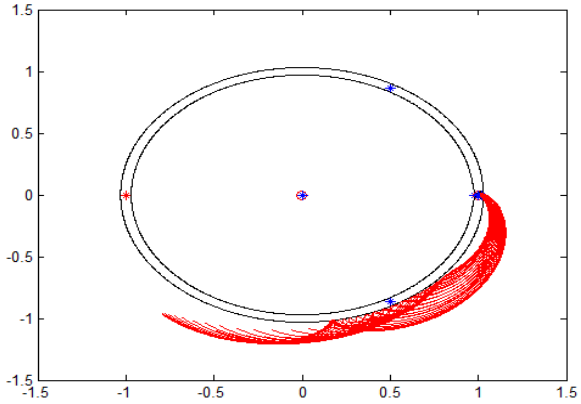

Figure 3.11: L_2 Right Unstable Manifold

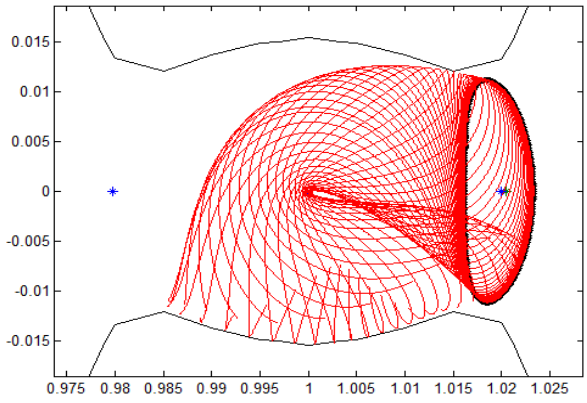

Figure 3.12: L_2 Left Unstable Manifold

In spite of low energy consumption, another beneficial aspect of the manifold surface is that all the branches of the manifolds intersects at the Lyapunov orbit.

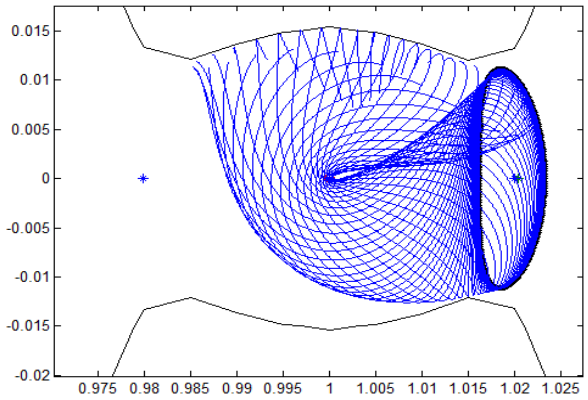

Figure 3.13: L_2Left Stable Manifold

Moreover, when the manifolds intersect each other a manifold to manifold transfer is possible, if appropriate incremental velocity is provided. When the manifolds intersect in the phase space, they meet at same positions but with different velocities. But to perform a manifold to manifold transfer their velocities must be equal, for which a continuous thrust is provided by using propulsion systems(thrusters). This fact can be exploited to resolve the problem of exploring other planets by combining the low energy solutions of two PCRTBPs and system to system transfer through manifolds.The manifold surface contracts as the trajectories move towards the halo orbit a hence theoretically, no maneuver is necessary to transfer a spacecraft from a manifold to a periodic halo orbit.

3.5 Poincare Sections

Poincare sections are used to find initial condition for orbit with prescribed itineraries like a heteroclinic orbit.Intersection of the stable manifold of europa and unstable manifold of Ganymede on a common Poinacare section is used to find the patch point where a ΔV should be provided for a low energy transfer from Ganymede to Europa which will be described in detail in the next chapter.We adopt the following convention of Poincare Section for numerical construction in this work. Poinca sections are shown in figure.

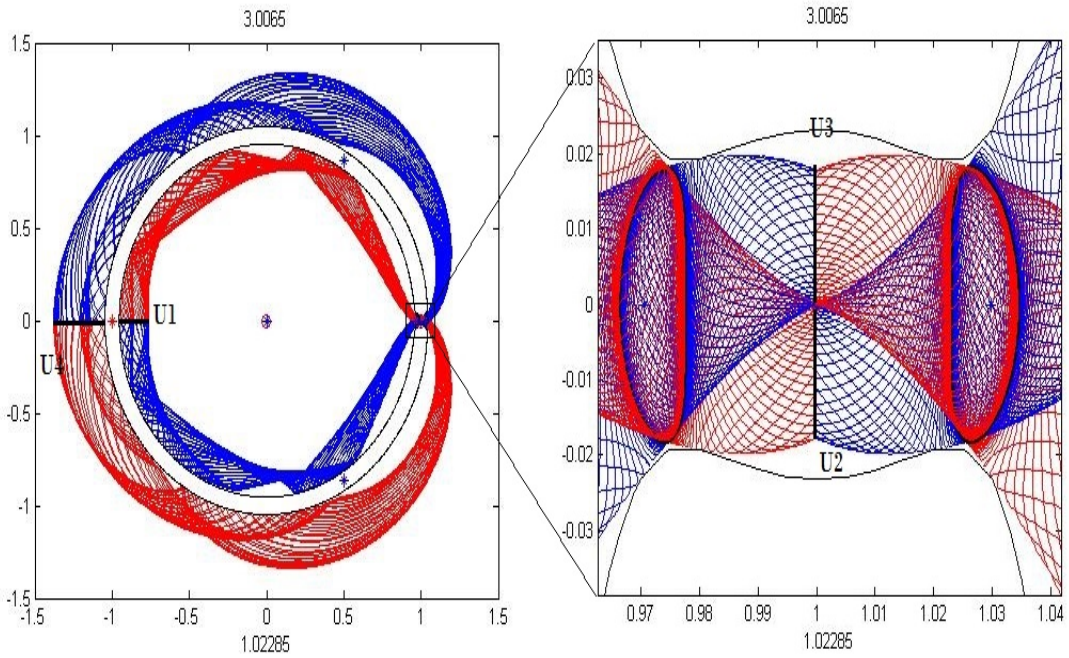

Figure 3.14: Poincare Sections

- The U_1 Poincare section will be the plane $y = 0; x < 0$ in the interior region.
- The U_2 section will be the plane $x = 1 - \mu; y < 0$ moon region.
- The U_3 section will be the planes $x = 1 - \mu; y > 0$ in the moon region.
- The U_4 Poincare section will be the plane $y = 0; x < -1$ in the exterior region.

3.6 Homoclinic Trajectory

The homoclinic trajectory is in the intersection of the stable and unstable manifolds of the periodic orbit. A homoclinic orbit is an orbit that connects a periodic orbit of a libration point to itself. Homoclinic orbits exists both in the interior and exterior realms. These are the orbits which are both forward and backward asymptotic to an unstable Lyapunov orbit.The intersections of stable and unstable manifolds of L_1 and L_2 periodic orbits is used to determine transversal homoclinic orbits in both the interior and exterior realms.

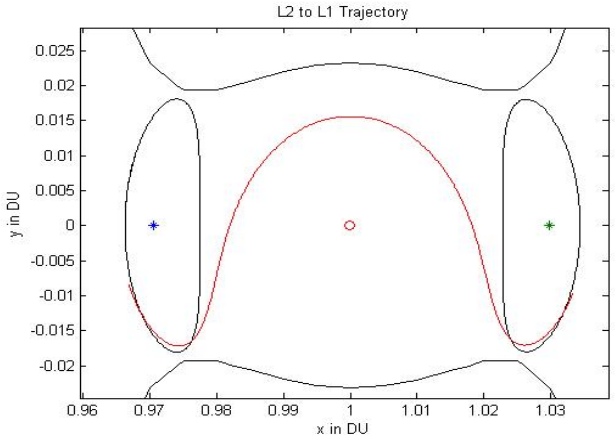

Figure 3.15: Heteroclinic Trajectory

3.7 Heteroclinic Trajectory

A heteroclinic trajectory, also known as a heteroclinic connection, is an orbit lying in the intersection of the stable manifold of one periodic orbit and the unstable manifold of another periodic orbit. A heteroclinic orbit is an orbit that connects a periodic orbit of a one libration point to periodic orbit of another libration point. The intersections of stable manifold of L_2 and unstable manifold of L_1 is used to determine transversal heteroclinic orbits in the Jupiter realm which connect asymptotically the L_1 and L_2 Lyapunov orbits.

3.8 Conclusion

This chapter dealt with generation of manifolds. By systematically seeking heteroclinic connections between Lagrange point orbits of adjacent moons,we can design trajectories which transfer from the vicinity of one moon to another using little fuel. One can seek intersections between the channels of transit orbits enclosed by the stable and unstable manifold tubes of Lyapunov orbits of different moons using the method of Poincare section. With maneuvers sizes Δv much smaller than that necessary for Hohmann transfers, transfers between moons are possible.This is explained in next chapter.

Chapter 4

The Galilean Moon System

4.1 Introduction

The Galilean moons are the four moons of Jupiter discovered by Galileo Galilei around January 1610. They are the largest of the moons of Jupiter and are Lo, Europa, Ganymede, and Callisto. They are among the most massive objects in the Solar System outside the Sun and the eight planets, with radii larger than any of the dwarf planets. The three inner moons Ganymede, Europa, and Lo, participate in a 1:2:4 orbital resonance.

Lo is the innermost of the four Galilean moons of Jupiter and, with a diameter of 3,642 kilometers, the fourth largest moon in the Solar System.With over 400 active volcanoes, Lo is the most geologically active object in the Solar System. Its surface is dotted with more than 100 mountains. Lo is primarily composed of silicate rock surrounding a molten iron or iron sulfide core. Although not proven, recent data from the Galileo orbiter indicate that Lo might have its own magnetic field. Lo has an extremely thin atmosphere made up mostly of sulfur dioxide SO_2

Europa, the second of the four Galilean moons, is the second closest to Jupiter and the smallest at 3121.6 kilometers in diameter, which is slightly smaller than the Moon. It is one of the smoothest objects in the solar system, with a layer of water surrounding the mantle of the planet, thought to be 100 kilometers thick.The smooth

surface includes a layer of ice, while the bottom of the ice is theorized to be liquid water. The apparent youth and smoothness of the surface have led to the hypothesis that a water ocean exists beneath it, which could conceivably serve as an abode for extraterrestrial life. Heat energy from tidal flexing ensures that the ocean remains liquid and drives geological activity. Life may exist in Europa's under-ice ocean, perhaps subsisting in an environment similar to Earths deep-ocean hydro thermal vents or the Antarctic Lake Vostok. Life in such an ocean could possibly be similar to microbial life on Earth in the deep ocean. So far, there is no evidence that life exists on Europa, but the likely presence of liquid water has spurred calls to send a probe there.Europa is primarily made of silicate rock and likely has an iron core. It has a tenuous atmosphere composed primarily of oxygen.

Ganymede, the third Galilean moon is the largest natural satellite in the Solar System at 5262.4 kilometers in diameter, which makes it larger than the planet Mercury - although only at about half of its mass since Ganymede is an icy world. It is the only satellite in the Solar System known to possess a magnetosphere, likely created through convection within the liquid iron core. Ganymede is composed primarily of silicate rock and water ice, and a salt-water ocean is believed to exist nearly 200 km below Ganymede's surface, sandwiched between layers of ice.The metallic core of Ganymede suggests a greater heat at some time in its past than had previously been proposed. The surface is a mix of two types of terrain highly cratered dark regions and younger, but still ancient, regions with a large array of grooves and ridges. Ganymede has a high number of craters, but many are gone or barely visible due to its icy crust forming over them. The satellite has a thin oxygen atmosphere that includes O, O_2, and possibly O_3 (ozone), and some atomic hydrogen.

Callisto is the fourth and last Galilean moon, and is the second largest of the four, and at 4820.6 kilometers in diameter, it is the third largest moon in the Solar System. It does not form part of the orbital resonance that affects three inner Galilean satellites and thus does not experience appreciable tidal heating. Callisto is composed

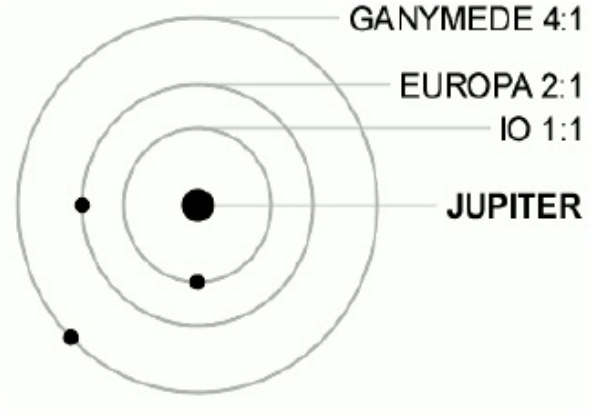

Figure 4.1: Orbital Resonance of Galilean Moons

of approximately equal amounts of rock and ices, which makes it the least dense of the Galilean moons. Callisto is surrounded by an extremely thin atmosphere composed of carbon dioxide and probably molecular oxygen. Investigation revealed that Callisto may possibly have a subsurface ocean of liquid water at depths greater than 100 kilometers. The likely presence of an ocean within Callisto indicates that it can or could harbor life. However, this is less likely than on nearby Europa. Callisto has long been considered the most suitable place for a human base for future exploration of the Jupiter system since it is furthest from the intense radiation of Jupiter.

Searching for life in other parts of the universe is a way of answering questions about ourselves.To reach that goal,a space mission is necessary that can obtain spectra of exoplanets atmospheres.Europa,one of Galilean moon of Jupiter is thought to be a hospitable to life because of vast liquid ocean that may existing under its icy crust.Low Energy trajectories which take full advantage of the natural dynamics are, now used to design successful and efficient missions. In this chapter numerical computations of trajectories in Galilean Moon System are discussed.The trajectory consists of 3 sections where it starts from beyond Ganymede,captured temperoryly by Ganymede, then transferred to Europa where it is ballistically captured by Europa. A trajectory from exterior realm of Ganymede to interior realm is designed first. During this transfer, the spacecraft could orbit Ganymede or could execute a flyby, both of which

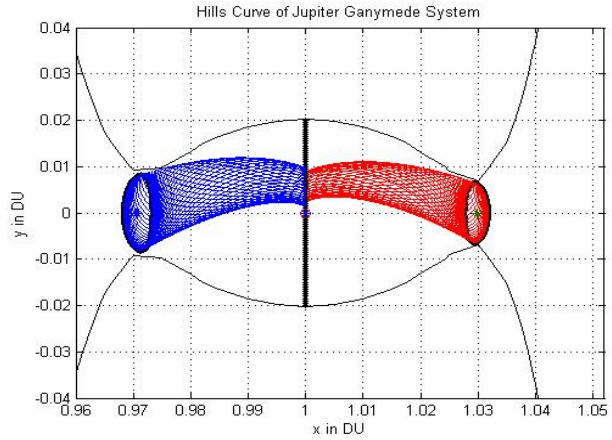

Figure 4.2: Poincare Intersection of L_2 unstable manifold and L_1 stable manifold for C=3.0074

are discussed. Then an end to end trajectory from a jovicentric orbit beyond the orbit of Ganymede to a ballistic capture orbit around Europa.Algorithm and Simulation results for both trajectories are presented in most simplest manner.

4.2 Trajectory from L_2 to L_1 of Ganymede

The primary objective is to find a *low energy trajectory*, which begins at L_2 periodic orbit(or in the exterior realm) and ends at L_1 periodic orbit(or interior realm). An unstable manifold of L_2 periodic orbit and a stable manifold of L_1 periodic orbit is designed. The energy or Jacobi constant is chosen as same value so as to produce a zero Δv trajectory. Start with a large number of initial points in the four-dimensional phase space, and save only those whose orbits correspond with this itinerary. The search could be simplified tremendously by considering tube dynamics on an energy surface. Then the search becomes, one of searching for an area, on a two-dimensional Poincare section for which all the points in that area correspond to an initial condition with this itinerary.

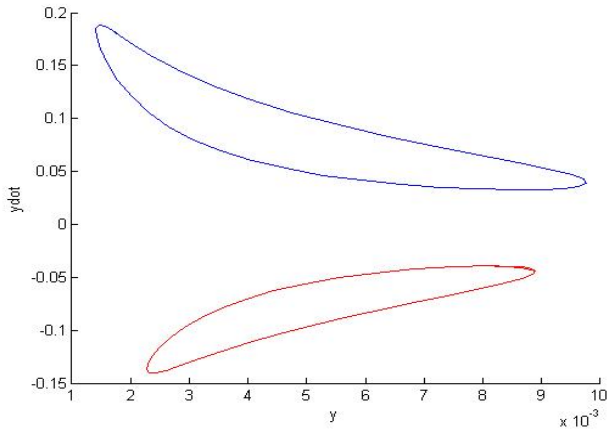

Figure 4.3: $(y_0, \dot{y}_0)$ curve for C=3.0074

4.2.1 Algorithm for L_2 to L_1 trajectory

1. Select an Appropriate Energy or Jacobi constant Value such that $E_2 < E < E_3$ or$C_2 > C > C_3$ so that both L_2 and L_1 necks are open.

2. Compute the location of the Equilibrium Points by solving dynamic equations.

3. Compute the Periodic Orbits around L_1 and L_2 Using Differential correction procedure.Same energy is chosen for L_2 and L_1 orbits.

4. Compute the Invariant Manifolds. Unstable manifold of L_2 periodic orbit and a Stable manifold of L_1 periodic orbit is generated.

5. An appropriate Poincare Section(Poincare Cut) is chosen and intersection of manifolds at Poincare section is analyzed. The first intersection of manifolds at Poincare section is used to design a flyby trajectory and further intersections are used to generate trajectory that orbit Ganymede.

6. Consider Tube Dynamics to Compute the Desired Initial Condition. Poincare section is chosen such that one of phase variable is either constant or could be obtained easily using Poincare section. The next two variables are obtained from intersection of manifolds at Poincare section. Since Jacobi constant **C** is same, the fourth variable is found from Jacobi equation.

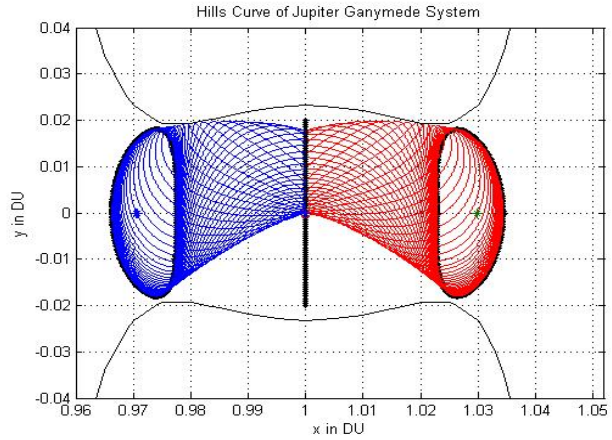

Figure 4.4: First Poincare Intersection of L_2 unstable manifold and L_1 stable manifold for C=3.0065

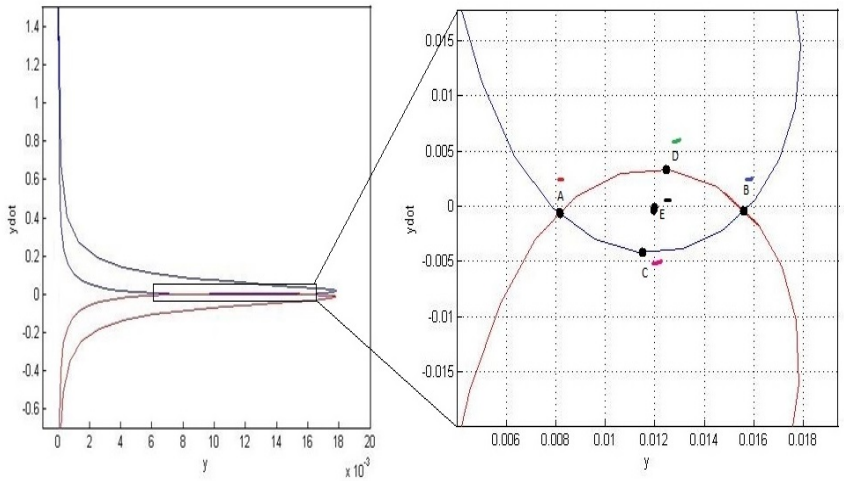

Figure 4.5: $(y_0, \dot{y_0})$ curve for C=3.0065

7. Numerically Integrate the Initial Condition obtained in previous step, backward and forward, to obtain required trajectory.

Since we need a transfer from L_2 to L_1, we take L_2 unstable manifold as well as L_1 stable manifold.Poincare section U_3. Intersection of above manifolds at Poincare section is found out.Now initial conditions are found. Since U_3 is chosen,$x_0 = 1 - \mu$. $(y_0, \dot{y_0})$ are chosen from Poincare Section. $\dot{x_0}$ is obtained from Energy equation. The initial condition obtained is integrated forward and backward to obtain required trajectory.it should be noted that , if there is NO intersection of manifolds on Poincare

section, C value is varied until an intersection is obtained.

4.2.2 Zero ΔV Fly By Trajectory

Initially value of Jacobi Constant, C is chosen as 3.0074 (Fig 4.1). The $(y_\dot{y})$curve does not intersect, hence a zero ΔV trajectory is not possible. Value of C is now decreased to 3.0065(Fig 4.3). Zero ΔV trajectories are generated using initial conditions obtained from $(y_\dot{y})$curves. Different initial conditions(A,B,C,D,E) are obtained from Poincare section and each initial condition produces different trajectories. The trajectories generated may wound on to both periodic orbits, or any one of them, or may go to interior or exterior realms through periodic orbits. As shown in Fig(4.5), trajectories generated from initial conditions at point A and B wound on to both L_1 and L_2 periodic orbit since both these points are on $(y\_\dot{y})$ curves of L_1 stable manifold and L_2unstable manifold. Similarly trajectories generated from initial conditions at point C and D wound on to L_1 and L_2 periodic orbits respectively. Finally trajectories generated from initial conditions at point E moves to interior and exterior realm (Fig 4.5). None of the trajectories orbit Ganymede here.

4.2.3 Zero ΔV Trajectory orbiting Ganymede

In order to have a trajectory that orbit Ganymede during its travel from L_2 to L_1, Poincare section U_3 is chosen and the intersection of above manifolds at Poincare section is obtained. Since U_3 is chosen,$x_0 = 1 - \mu$. $(y_0, \dot{y_0})$ are chosen from Poincare Section. $\dot{x_0}$ is calculated from Jacobi Integral equation. The value of C is chosen as 3.0070 (Fig 4.6) and $(y_\dot{y})$curve intersect. Using same analysis in section 4.2.2 trajectories that wound on to different points after orbiting Ganymede is found.

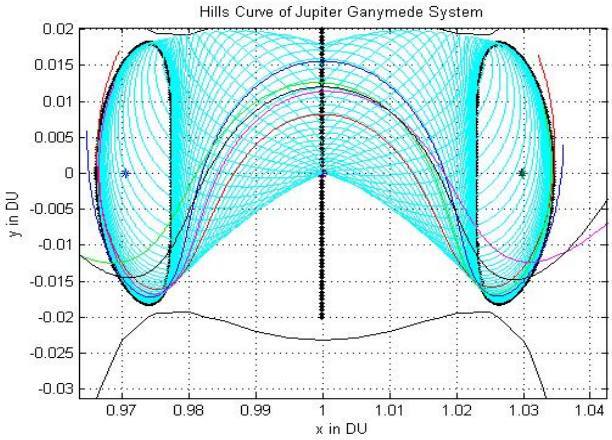

Figure 4.6: Heteroclinic Trajectories

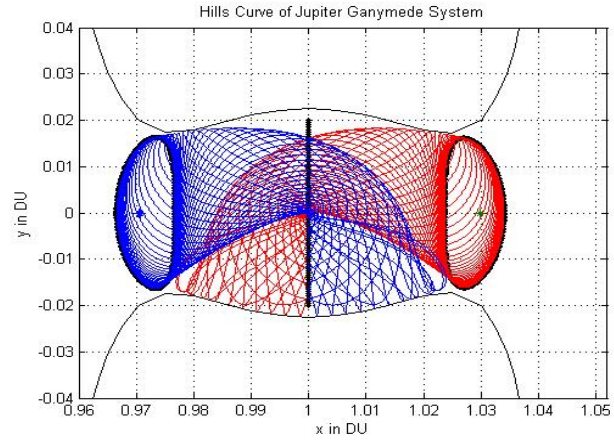

Figure 4.7: Second Poincare Intersection of L_2 unstable manifold and L_1 stable manifold for C=3.0065

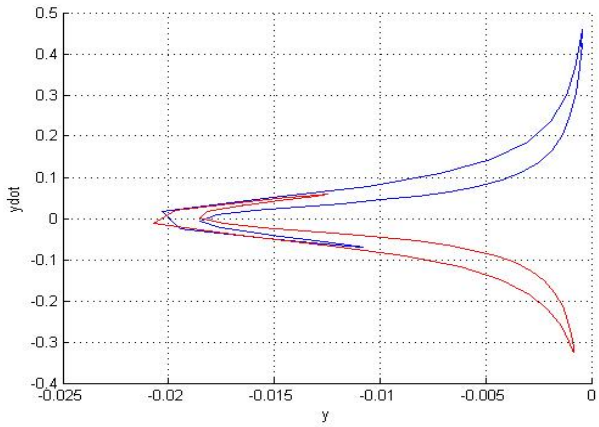

Figure 4.8: $(y_0, \dot{y_0})$ curve for C=3.0065

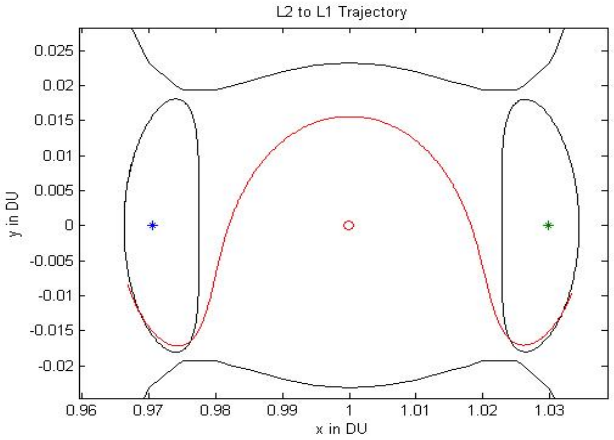

Figure 4.9: L_2 to L_1 Transfer flyby trajectory

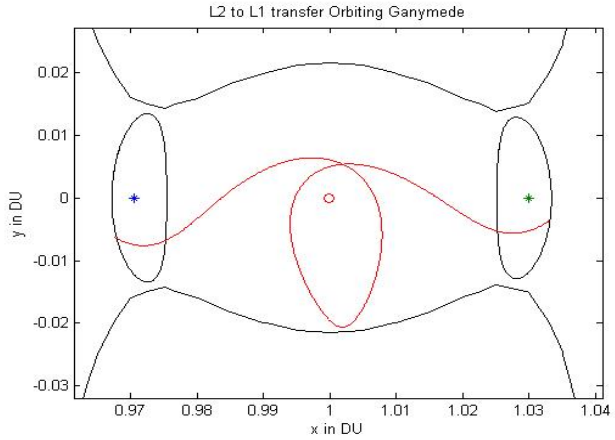

Figure 4.10: $L_2$to L_1 Transfer, temperorily captured by Ganymede

4.3 Trajectory for Ganymede to Europa Transfer

The trajectory begins at L_1 periodic orbit of Ganymede and ends at $L_{21}2$ periodic orbit of Europa where it is ballistically captured. Left unstable manifold of Ganymede and a right stable manifold of Europa is designed. The Jacobi constant are different for moth manifolds since both are in their respective rotating frame. To effect a Ganymede to Europa transfer with a ballistic capture at Europa[4] following procedure is followed.

4.3.1 Algorithm for Ganymede to Europa transfer trajectory

1. Treat the Jupiter-Ganymede-Europa-spacecraft 4-body problem as two coupled circular restricted 3-body problems, Jupiter-Ganymede-spacecraft and Jupiter-Europa spacecraft systems.

2. Use unstable manifolds of periodic Lyapunov orbits about the Jupiter-Ganymede Lagrange points to provide a low energy transfer from Ganymede, to the stable manifolds of periodic orbits around the Jupiter- Europa Lagrange points.

3. Use the stable manifolds of the periodic orbits around the Jupiter-Europa Lagrange points to provide a ballistic capture about Europa.

The construction is done mainly in the Jupiter-Europa rotating frame using a Poincare section which helps to connect the Jupiter-Ganymede libration point trajectory with the Europa ballistic capture trajectory. We start with the PCR3BP model to compute the invariant manifolds and use them to construct the Jupiter-Ganymede libration point trajectory and the Europa ballistic capture trajectory.From the transfer patch point and integrate forward and backward in time to obtain trajectory towards each moon's vicinity.We compute Jupiter-Ganymede invariant unstable manifolds of an L_1 periodic orbit (interior region) and Jupiter-Europa invariant stable manifolds of an L_2 periodic orbit (exterior region).We look at the intersection of these manifolds on a common Poincare section. The sections chosen are U_4 section of the Jupiter-Europa rotating frame and U_1 section of the Jupiter-Ganymede rotating frame. The phase of Ganymede is chosen such that this plane coincides with the U_4 section of the Jupiter-Europa rotating frame at the time of the transfer maneuver. A different Phase of Ganymede may be chosen if there is no intersection of $(x, \dot{x})$ or $(x, \dot{y})$ curves.

Jupiter-Europa rotating frame is chosen as preferred frame of reference. Thus, the Europa manifold, or the Europa channel, is time invariant.Now Transform U_1 section of the Jupiter-Ganymede rotating frame to Jupiter-Europa rotating frame so as to

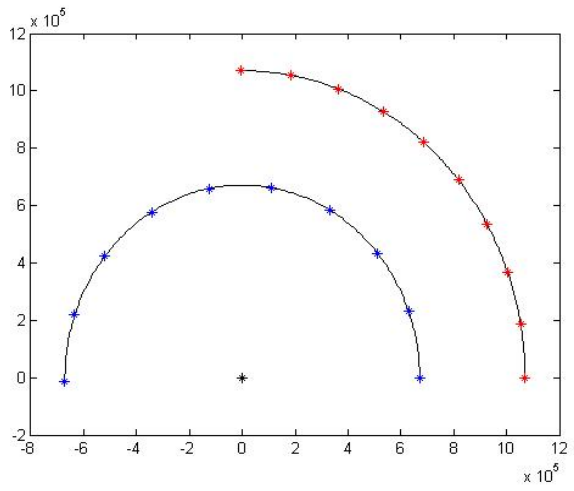

Figure 4.11: Ganymede and Europa trajectory in inertial frame

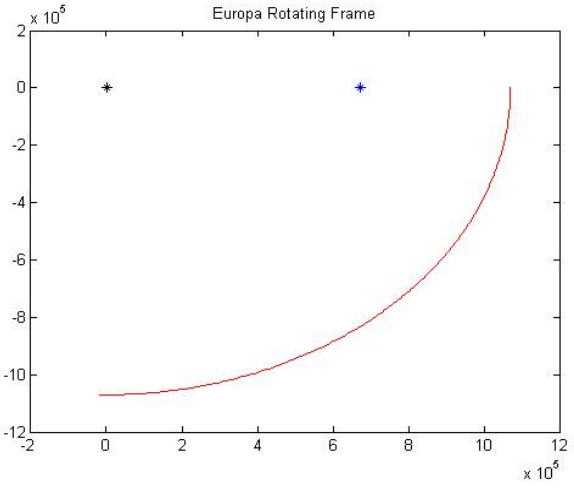

Figure 4.12: Ganymede trajectory in Europa rotating frame

look for intersections between the Europa and Ganymede channels. This is simply a re scaling of the coordinates. Ganymede moves in a circular retrograde orbit as seen in Europa's rotating frame and hence Ganymede's channel is time dependent.

4.3.2 Coordinate transformations between rotating frames

Since Jupiter-Europa rotating frame is chosen as reference frame, manifold in Jupiter-Ganymede rotating frame should be transformed to Jupiter-Europa rotating frame. Transforming Ganymede and Europa to inertial frame results in circular orbit, in anticlockwise direction. As mentioned in introduction,Ganymede, Europa, and Lo,

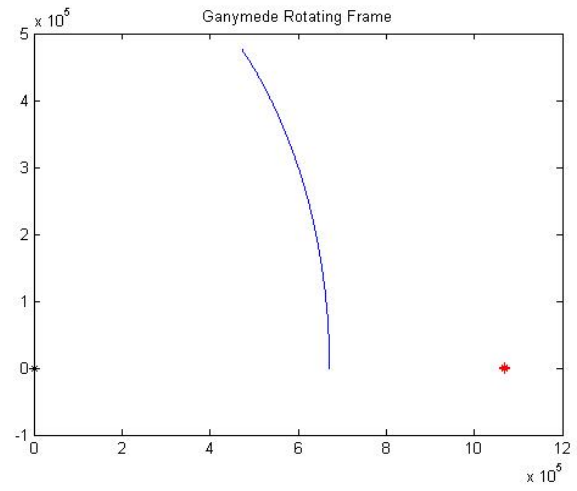

Figure 4.13: Europa trajectory in Ganymede rotating frame

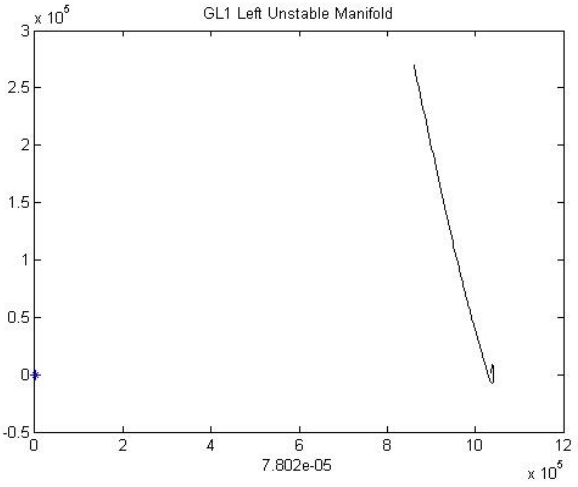

Figure 4.14: Ganymede manifolds in Ganymede rotating frame

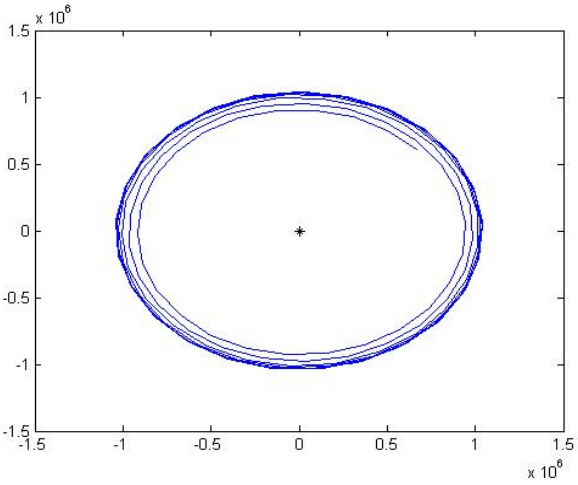

Figure 4.15: Ganymede manifolds transformed to Inertial frame

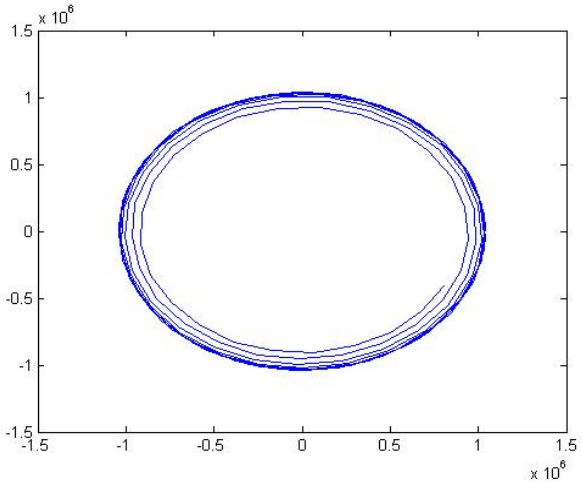

Figure 4.16: Ganymede manifolds transformed to Europa rotating frame

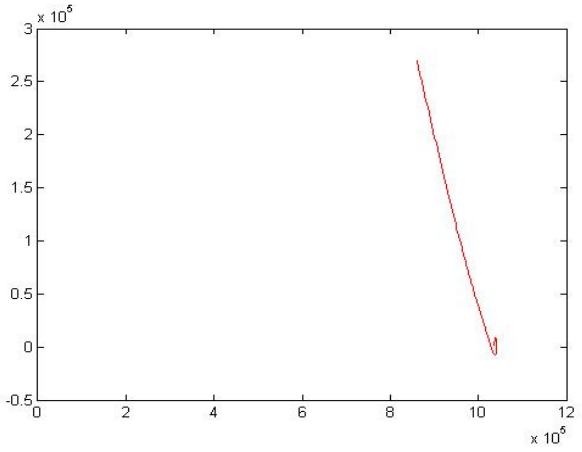

Figure 4.17: Ganymede manifolds transformed from Inertial back to Ganymede rotating frame

participate in a 1:2:4 orbital resonance, angular velocity of Europa is twice that of Ganymede. So Europa travel twice as that of Ganymede during same time.This is depicted in fig 4.11. Europa remains fixed in Europa rotating frame and transforming Ganymede into Europa frame results in a clockwise trajectory of Ganymede. This is the case with Ganymede manifolds also, only difference is that the trajectory may not be exactly circular. Similarly transforming Europa into Ganymede frame results in a anticlockwise trajectory. These are shown in fig 4.12 to 4.17. Transforming manifolds is complex, time consuming and computationally difficult. A more simpler approach is to transform Poincare section rather than transforming complete

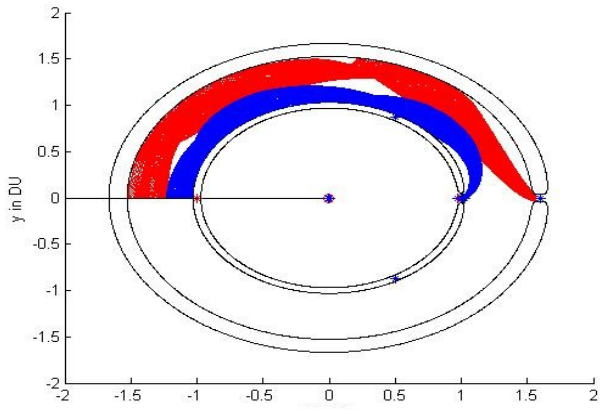

Figure 4.18: Ganymede Unstable Manifold and Europa Stable Manifold

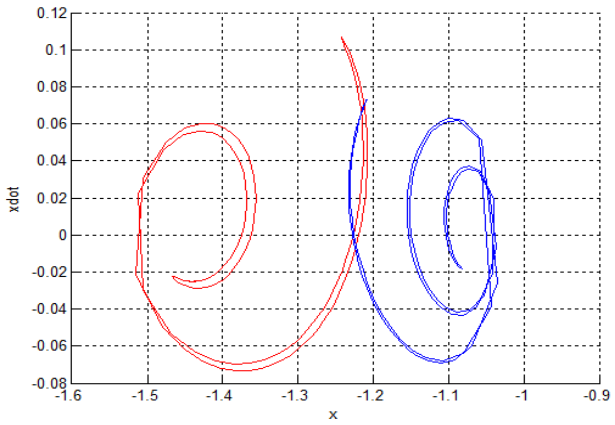

Figure 4.19: $(x, \dot{x})$ curve

manifolds. Coordinate Transformation discussed in section 2.5 is used.

4.3.3 Simulation Results

For numerical study, L_2 Lyapunov orbit with Jupiter-Europa Jacobi constant is chosen as$C_e = 3.0032$ and Ganymede L_1 Lyapunov orbit with Jupiter-Ganymede Jacobi constant$C_g = 3.050$ is chosen.Simulation results are shown in Figure 4.18 to Figure 4.21

The intersection around $(x = 1.218; x\_0 : 004)$ in Figure 4.6 proves that one can transit from Ganymede to Europa with no ΔV in the x-direction.But in Figure 4.7 for $x = 1.218$ we can see a significant gap between the Ganymede and Europa channels.

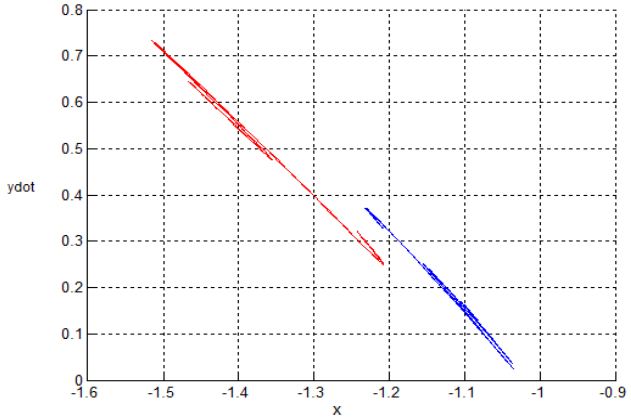

Figure 4.20: $(x, \dot{y})$ curve

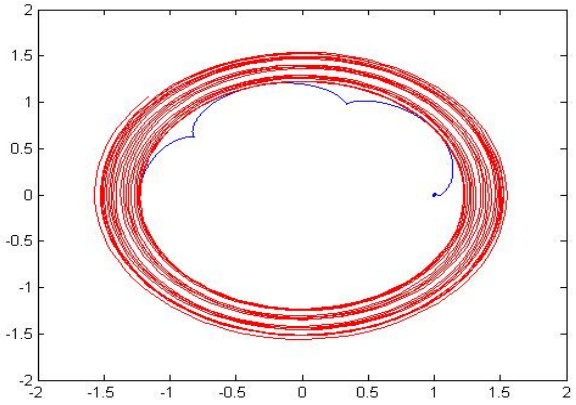

Figure 4.21: Ganymede to Europa trajectory in Europa Rotating frame

Therefore, a ΔV in the y-direction will be necessary. This is due to the fact that the Ganymede L_1 channel is not on the same Jupiter-Europa Jacobi constant surface as the Europa L_2 channel.The ΔV required is about 0.0870*13770=1198m/s at patch point to connect the two trajectories (i.e., forward capture by Europa and backward capture by Ganymede).Furthermore a ΔV of 124m/s,near Ganymede, is necessary to add one full loop around the moon. No ΔV ,was required for captured by Europa. Traditional Hohmann (patched 2-body) transfer from Ganymede to Europa requires a ΔV of 2822 m/s.

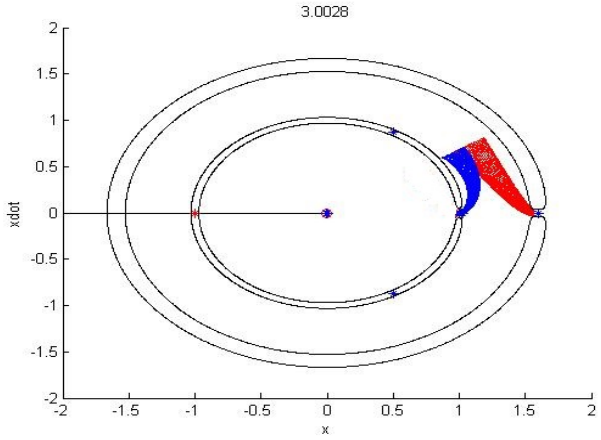

Figure 4.22: Zero Phasing of Ganymede

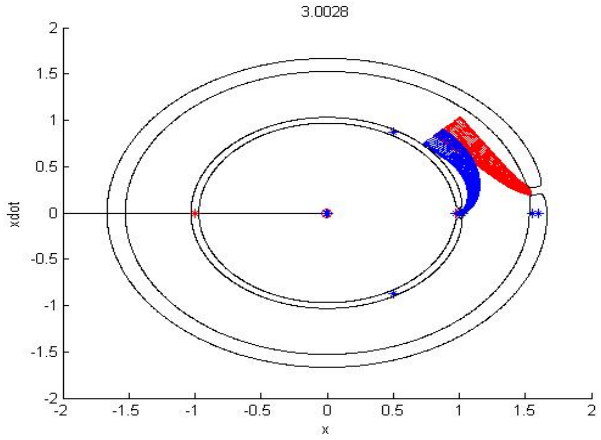

Figure 4.23: Negative Phasing of Ganymede

4.4 Optimisation of ΔV

Some approaches in order to reduce the value of ΔV is followed.

4.4.1 Phasing of Ganymede

The phase of Ganymede is chosen as zero for designing trajectory. Now phasing is introduced inorder to find, if trajectories with lower ΔV could be obtained. Unfortunately phasing did not provide any decrease in ΔV.

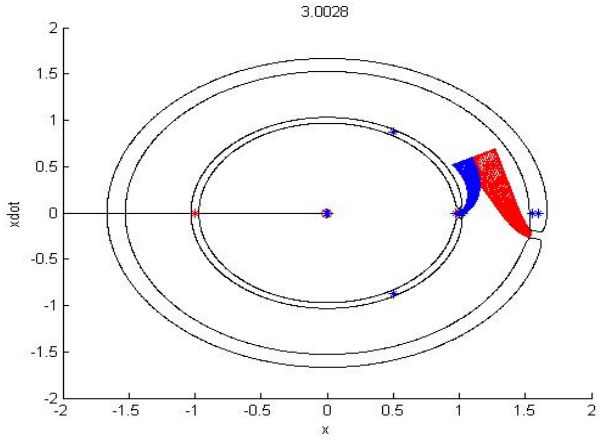

Figure 4.24: Positive Phasing of Ganymede

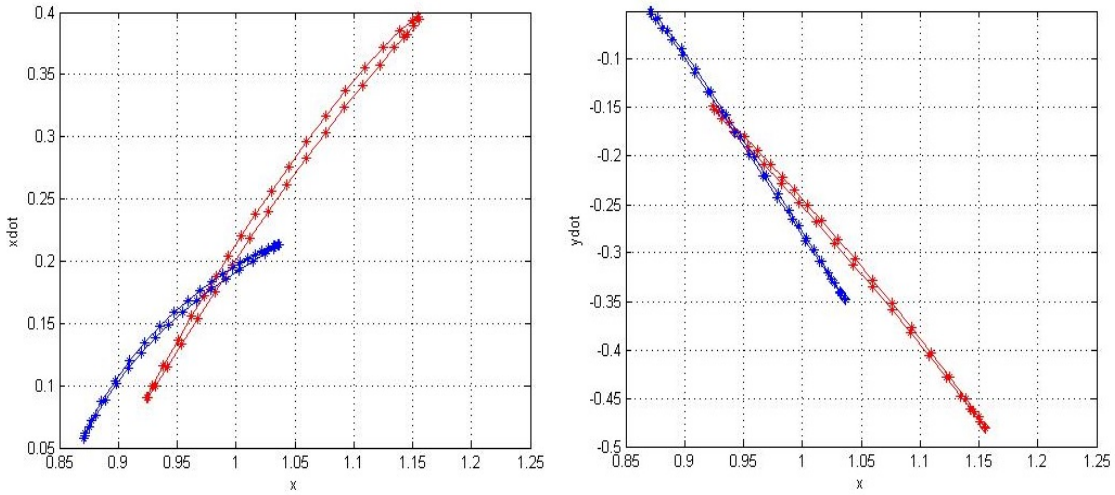

Figure 4.25: $(x, \dot{y})$ curve after positive Phasing of Ganymede

4.4.2 ΔV without using $(x, \dot{x})$ curves

The initial condition are found for different cases where manifolds intersect in position space. Other variables are found from numerical values obtained at Poincare section. In this case both $\dot{x}$ and $\dot{y}$ may be required. The lowest ΔV was found to be for trajectory with zero ΔV in x direction.

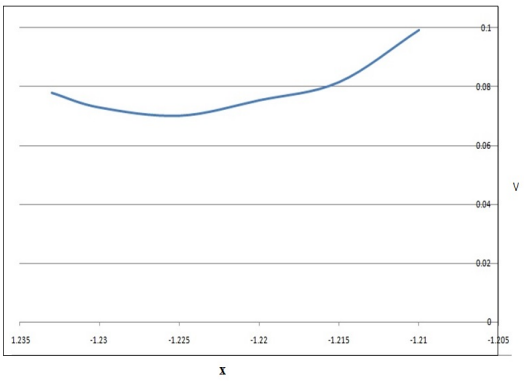

Figure 4.26: ΔV vs x

4.5 Conclusion

This chapter dealt with trajectories in Galilean moon system. Trajectories which transfer from the vicinity of one moon to another using little fuel is designed. One can seek intersections between the channels of transit orbits enclosed by the stable and unstable manifold tubes of Lyapunov orbits of different moons using the method of Poincare section. Combining trajectories generated in section 4.2 and 4.3 we can have a transfer from Ganymede to Europa. With maneuvers sizes Δv much smaller than that necessary for Hohmann transfers, transfers between moons are possible. This was also found to be the optimum value. Next chapter deals with a closed loop guidance using a non linear controller which is used for tracking and disturbance rejection.

Chapter 5

Dynamic Inversion Controller

5.1 Introduction

The PCRTBP is a nonlinear problem and highly dependent on initial condition. Dynamic equations are obtained and a controller based on the dynamic inverse is synthesized for the purpose of stabilization and trajectory tracking. Dynamic inversion achieve a specified dynamic response by using a feedback signal to cancel inherent dynamics.

5.2 Dynamic Inversion

Consider a non-linear time invariant system described by the following equations

$$\dot{X} = f(X) + g(X)U \tag{5.1}$$

$$Y = h(X) \tag{5.2}$$

where, X is the state vector, U is the control vector, f and g are scalar functions and Y is the output vector. If the system is affine in the controls, then solving for the control vector yields

$$U = g^{-1}(X)(\dot{X} - f(X)) \tag{5.3}$$

Inherent dynamics is replaced by desired dynamics. Different forms of desired dynamics will respond differently with same disturbances. Selection of desired dynamics form should be such that, it will satisfy specified performance and robustness requirements. The proportional-derivative form was used whose dynamics is given by,

$$V = K_1(X_a - X_d) + K_2(\dot{X}_a - \dot{X}_d) \tag{5.4}$$

Dynamic inversion control is used by trajectory tracker is to track the final manifold (reference manifold) from a point on the initial manifold.The dynamics of the spacecraft given by

$$\ddot{x}_{sc} = f_1(x_{sc}, \dot{y}_{sc}) + g_1 u_x \tag{5.5}$$

$$\ddot{y}_{sc} = f_1(y_{sc}, \dot{x}_{sc}) + g_2 u_y \tag{5.6}$$

where u_x and u_y are control signal in x and y direction. The virtual input V is given by

$$V_x = \ddot{x}_d - K_1(X_a - X_d) + K_2(\dot{X}_a - \dot{X}_d) \tag{5.7}$$

Substituting this in eq 5.5 we get

$$\ddot{x}_{sc} = \ddot{x}_d - K_1(X_a - X_d) + K_2(\dot{X}_a - \dot{X}_d) \tag{5.8}$$

Rearranging eq 5.8 we get

$$\ddot{e}_x + k_1\dot{e}_x + k_2 e_x = 0 \tag{5.9}$$

where e_x is position error in x direction. For error dynamics to have a second order

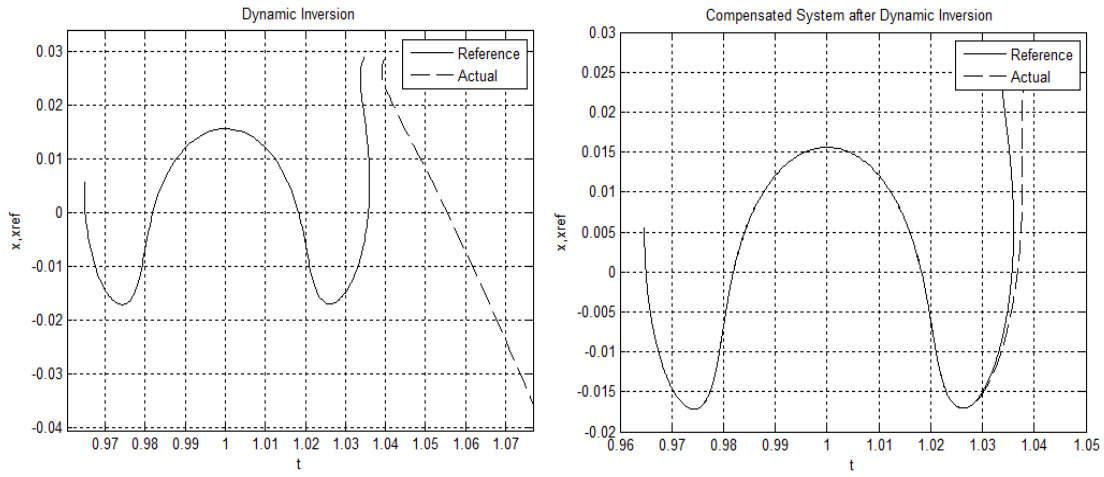

Figure 5.1: Dynamic Inversion Control

response with damping ratio ζ and natural frequency ω_n,

$$k_1 = 2\zeta\omega_n$$

$$k_2 = \omega_n^2$$

The value of ζ is taken to be 0.8 and that of ω_n as 2.5Hz which gives settling time $t = 2T$

The control signal in x direction by dynamic inversion is given by

$$u_x = g_1^{-1}[V_x - f_1(y_{sc}, \dot{x}_{sc})] \tag{5.10}$$

Similarly the control signal in y direction is given by

$$u_y = g_2^{-1}(V_y - f_2(y_{sc}, \dot{x}_{sc})) \tag{5.11}$$

5.3 Dynamic Inversion for L_2 to L_1 transfer

A reference trajectory was developed using algorithm given in section 4.2. From an initial trajectory in exterior region, NLDI controller is used to track reference

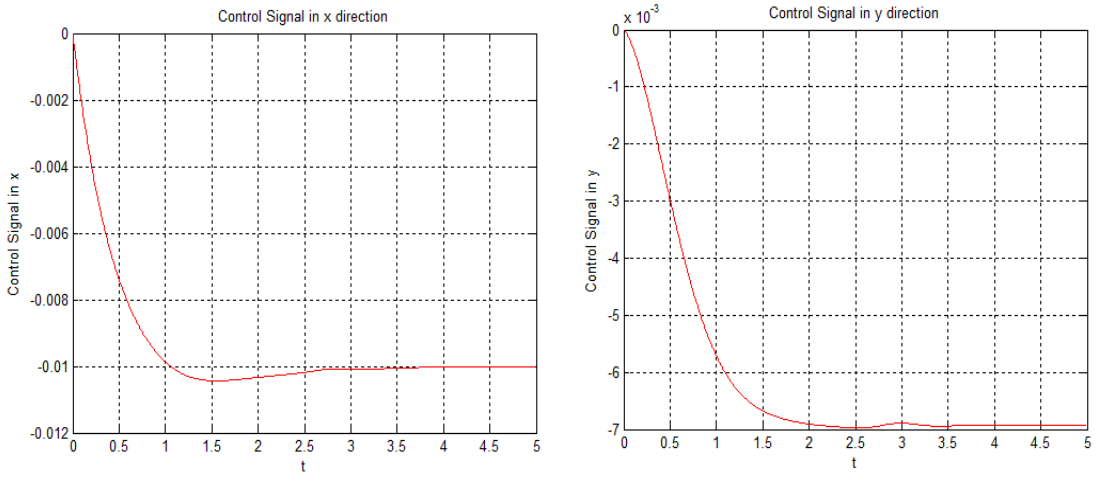

Figure 5.2: Control Signal in x and y direction

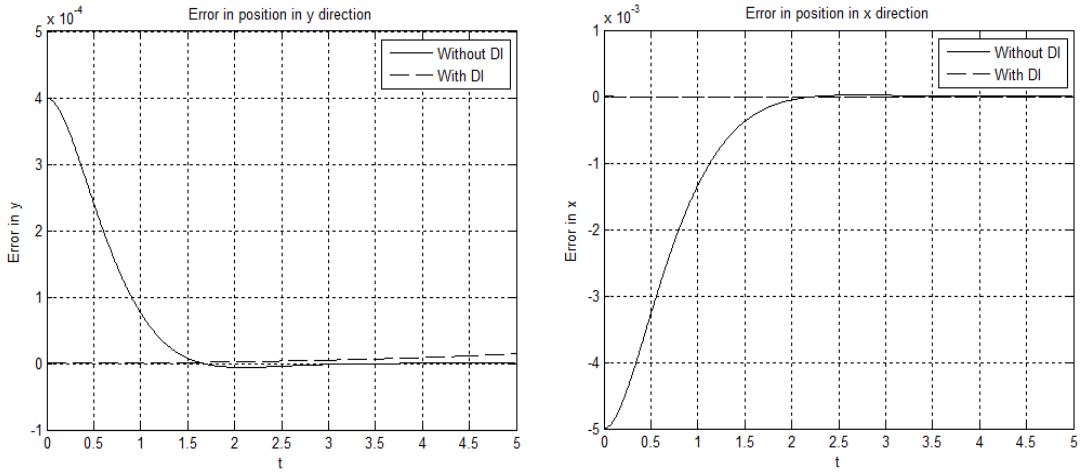

Figure 5.3: Position error in x and y direction

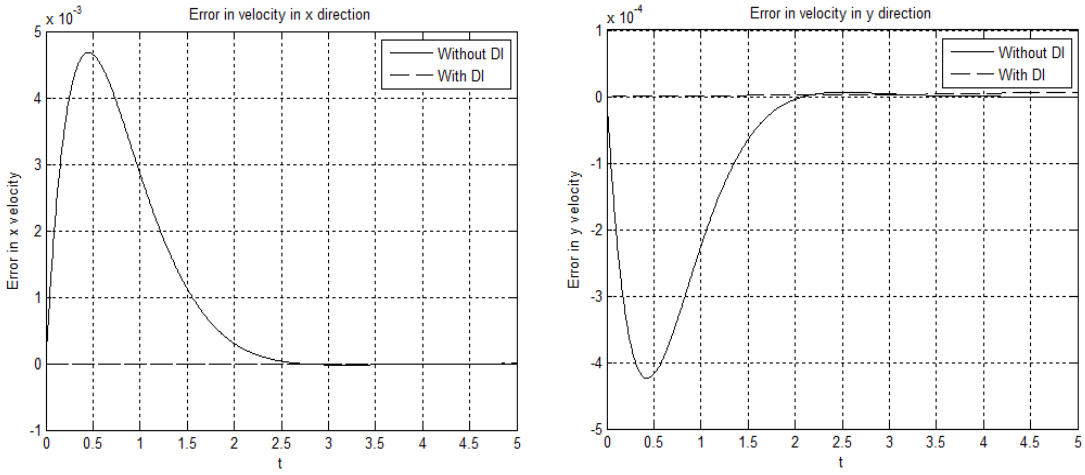

Figure 5.4: Velocity error in x and y direction

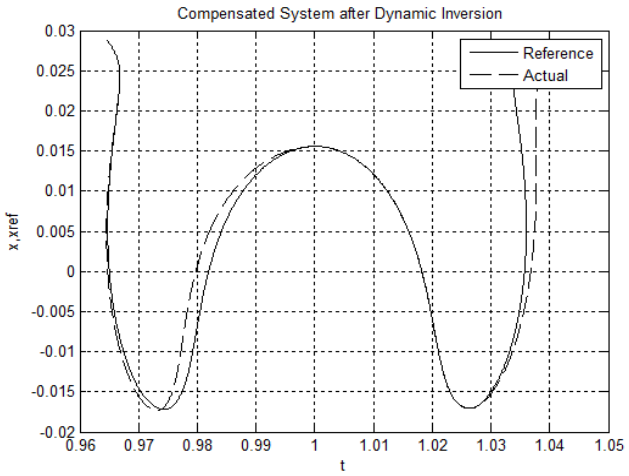

Figure 5.5: Dynamic Inversion Control with disturbance

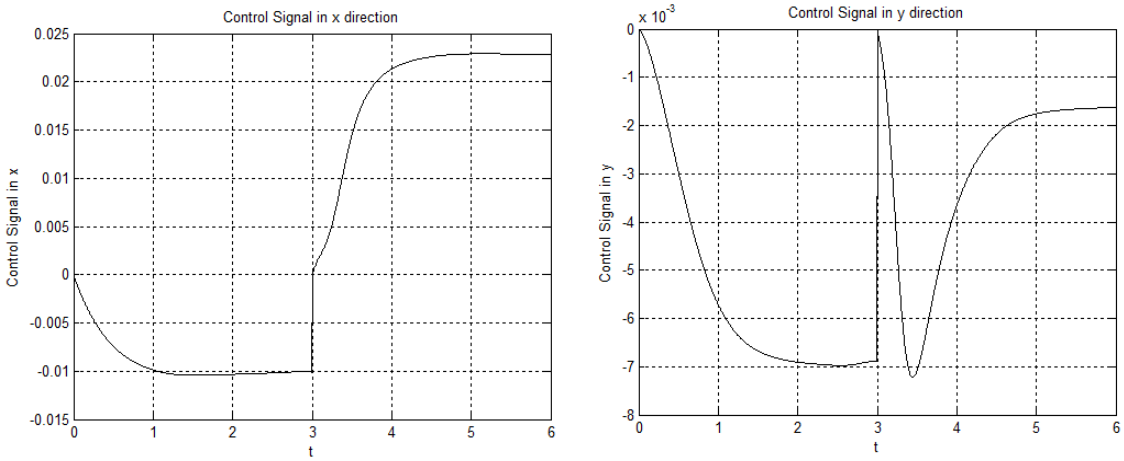

Figure 5.6: Control Signal in x and y direction

trajectory that will bring spacecraft to L_1 periodic orbit. Trajectory, control signal, position error and velocity error are shown in fig 5.1 to fig 5.4

5.4 Dynamic Inversion for L_2 to L_1 transfer with disturbance

A reference trajectory was developed using algorithm given in section 4.2. From an initial trajectory in exterior region, NLDI controller is used to track reference trajectory that will bring spacecraft to L_1 periodic orbit. Uncertainties and disturbances

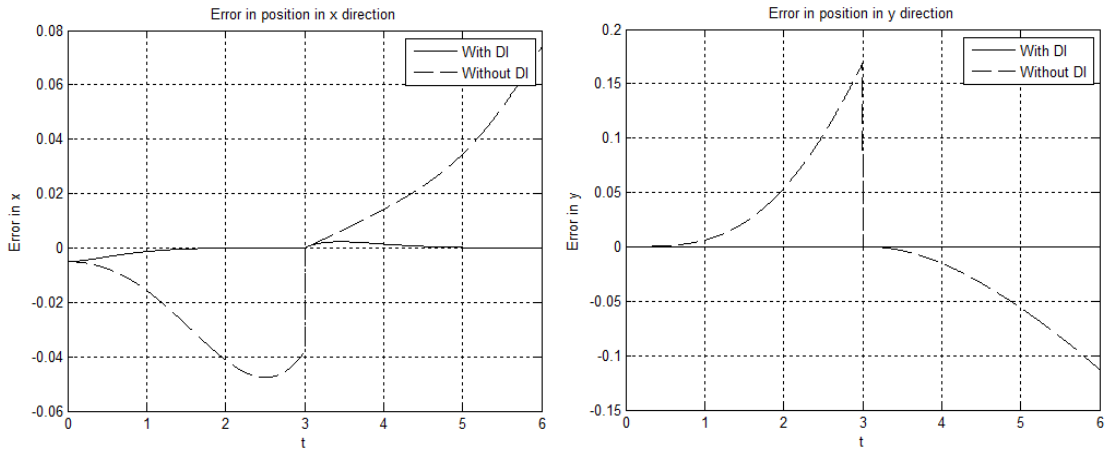

Figure 5.7: Position error in x and y direction

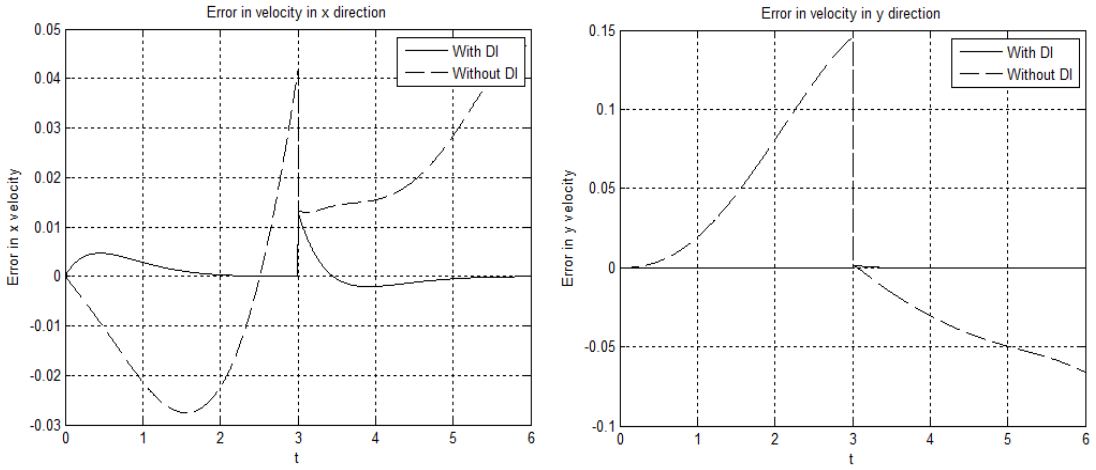

Figure 5.8: Velocity error in x and y direction

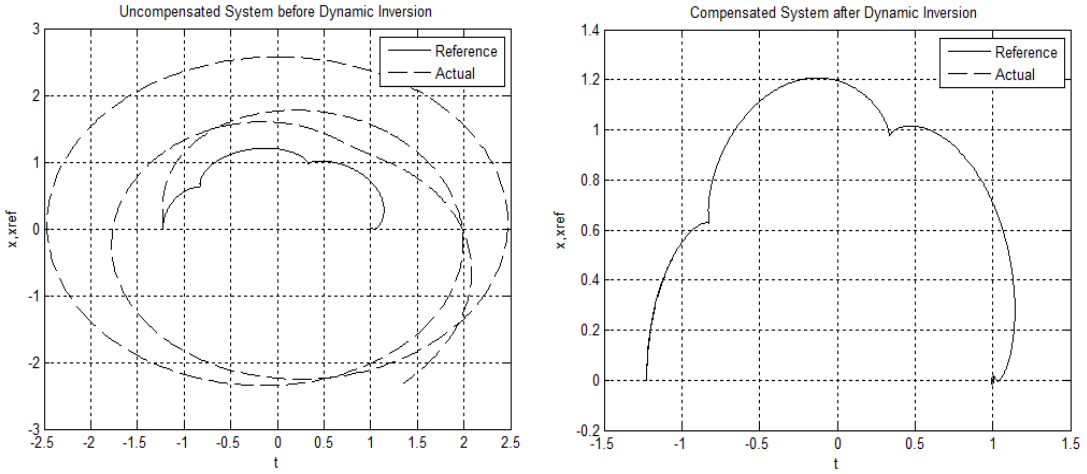

Figure 5.9: Dynamic Inversion Control

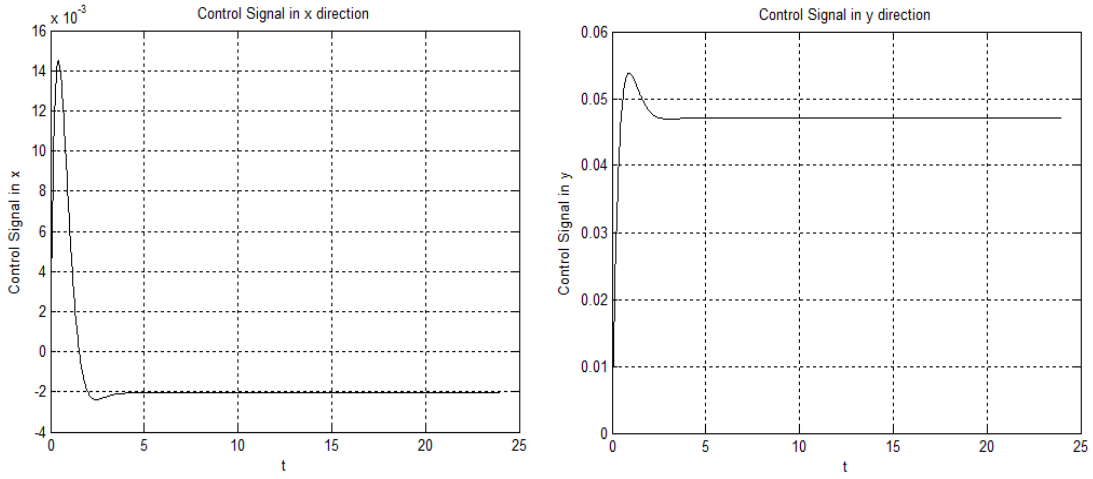

Figure 5.10: Control Signal in x and y direction

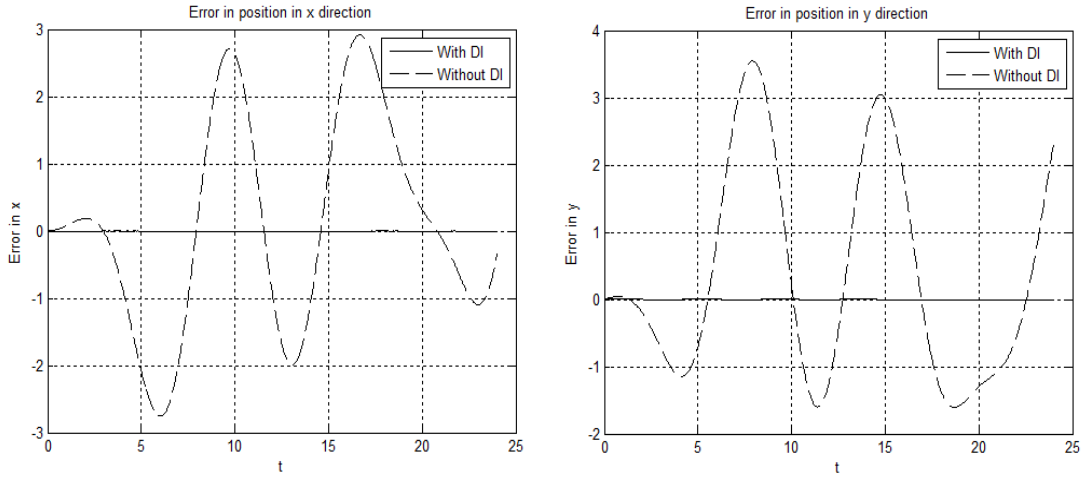

Figure 5.11: Position error in x and y direction

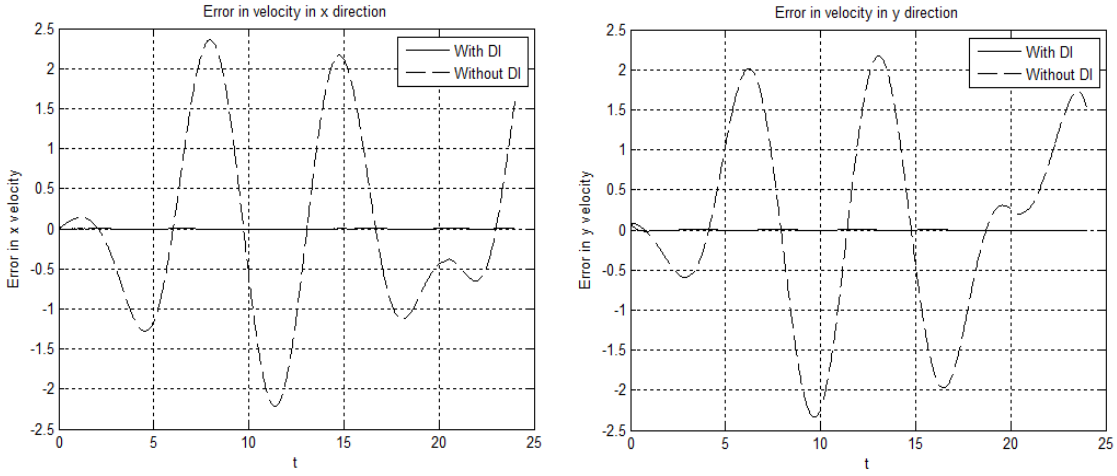

Figure 5.12: Velocity error in x and y direction

may occur due to reasons like solar radiation pressure. A perturbation is given, and spacecraft was able to track reference. Trajectory, control signal, position error and velocity error are shown in fig 5.5 to fig 5.8

5.5 Dynamic Inversion for Ganymede to Europa transfer

A reference trajectory was developed using algorithm given in section 4.3. Ganymede trajectory was generated till patch point. From an initial point at patch point, NLDI controller is used to track reference trajectory that will bring spacecraft to Europa. Trajectory, control signal, position error and velocity error are shown in fig 5.9 to fig 5.12

5.6 Conclusion

In this chapter a closed loop guidance was developed using Nonlinear dynamic inversion control. Reference trajectories were developed and a control law was formulated to track reference. Disturbances were included and spacecraft was able to track reference even in presence of disturbance.

Chapter 6

CONCLUSION

The dynamical systems techniques were used to investigate transport channels in the phase space which could be exploited by spacecraft to move from moon to moon within a planet's satellite system using low-fuel controls. This method of space mission design is an elaboration upon the patched conic approach, toward a patched 3-body approach. The delicate dynamics of the 4-body problem are well approximated by the coupled 3-body problem for a satellite system such as the Galilean moons of Jupiter. By systematically seeking heteroclinic connections between Lagrange point orbits of adjacent moons, one can design trajectories which transfer within the vicinity of one moon(exterior to interior region). The intersections between the channels of transit orbits enclosed by the stable and unstable manifold tubes of different moons using the method of Poincare section are utilized for transfer between moons. With maneuvers sizes Δv much smaller than that necessary for Hohmann transfers, transfers between moons are possible.

The problem is highly nonlinear and strongly dependent on initial condition. Continuous low thrust propulsion was used for trajectory correction maneuvers. A controller based on the dynamic inverse is synthesized for the purpose of stabilization and trajectory tracking.A reference trajectory was designed. The steering law was designed by using Nonlinear dynamic inversion control which successfully transferred a spacecraft to the reference manifold. The Error profiles at different time of flight

were analysed. The closed loop guidance algorithm developed provided satisfactory results under nominal and perturbed conditions.

6.1 Future Scope

Some of the recommendations for the extension of the work are

- Low energy earth moon transfer missions could be developed and continuous low thrust propulsion could be used to generate trajectories with any number of orbits around moon.
- Solar Sail applications could be added in Sun Jupiter bicircular model for Europa mission.
- Jupiter moon spacecraft 3 body problem could be extended as 4 body problem with Sun as major perturbing source.

REFERENCES

[**1** I. Newton,*The Principia: Mathematical Principles of Natural Philosophy*, University of California Press, 1999, Vol. 1. 2 Berkeley, California

[**2** V. Szebehely,*Theory of Orbits*, New Haven, Connecticut: Academic Press, first edition, 1967.

[**3** J. Barrow-Green,,*Poincare and the Three Body Problem*, vol. 11, History of Mathematics, Providence, Rhode Island: American Mathematical Society,1997.

[**4** L. Perko,*Differential Equations and Dynamical Systems*, New York: Springer-Verlag, 1891.

[**5** F. Moulton,*Periodic Orbits*, Institution of Washington 1920.

[**6**]W. S. Koon, M. W. Lo, J. E. Marsden, and S. D. Ross.: "Dynamical systems, the three- body problem and space mission design", *International Conference on Differential Equations*, Vol. 1. 2 (Berlin, 1999), pages 1167-1181

[**7**]M. W. Lo, W. S. Koon, J. E. Marsden, and S. D. Ross:' Heteroclinic connections between periodic orbits and resonance transitions in celestial mechanics, *Chaos*,427469, 2000.

[**8**] G. Comez, W. S. Koon, M. W. Lo: Invariant manifolds, the spatial three -body problem and space mission design, *American Astronautical Society*, PP 120, 2001

[**9**] Shane David Ross : Cylindrical Manifolds and Tube Dynamics in the Restricted Three -Body Problem, *California Institute of Technology*, Pasadena, California, April 2004.

[**10**]Martin.T.Ozimek : Cylindrical Manifolds and Tube Dynamics in the Restricted Three -Body Problem, *California Institute of Technology*,West Lafayette, Indiana, December 2006.

[**11**] W. S. Koon, M. W. Lo, J. E. Marsden, and S. D. Ross : Constructing a Low Energy Transfer Between Jovian Moons, *International Conference on Celestial Mechanics*,Evanston, IL, Dec. 1999.

[**12**] W.S. Koon, M. Lo, J. Marsden, S. Ross : Application of Dynamical Systems Theory to a Very Low Energy Transfer, *14th AAS/AIAA Space Flight Mechanics Conference*, Maui, Hawaii, February 8-12, 2004

[**13**]W.S. Koon, M. Lo, J. Marsden, S. Ross: Design of a multi-moon orbiter , *AIAA Space Flight Mechanics Meeting*, . Ponce, Puerto Rico. Paper No. AAS 03-143..

[**14**]W.S. Koon, M. Lo, J. Marsden, S. Ross: 'The InterPlanetary Superhighway and the Origins Program , *IEEE Aerospace Conference Proceedings*, Pasadena, (pp. 7-3543- 7-3562 vol.7).

[**15**]Ross, S., Grover, P:'Designing Trajectories in a Planet-Moon Enviornment Using the Controlled Keplerian Map. , *AIAA Space Flight Mechanics Meeting*, March 2009

[**16**]Strange, N., Longuski, J: 'Graphical Method for Gravity-Assist Trajectory Design , *AIAA Space Flight Mechanics Meeting*, January 2002

[**17**]C. C. Conley: Low energy transit orbits in the restricted three-body problems , *Journal on Applied Mathematics.*,November 1969

[**18**]Belbruno, E. A. and J. K. Miller:'Sun-perturbed Earth-to-Moon transfers with ballistic capture;*Journal of Guidance, Control and Dynamics*770-775,1993

[**19**]McGehee, R.: *Some homoclinic orbits for the restricted three-body problem*,PhD thesis, University of Wisconsin, Madison 1969

[**20**]Bate, R. R., D. D. Mueller, and J. E. White: *Fundamentals of Astrodynamics*,1971

[**21**]Farquhar, R: *The control and use of libration-point satellites*,PhD thesis, Stanford University, 1969

[**22**]E. Canalias, G. Gomez, M. Marcote, and J. J. Masdemont:' Assessment of mission design including utilization of libration points and weak stability boundaries, European Space Agency, 2004.

[**23**]M. Dellnitz, O. Junge, W. S. Koon, F. Lekien, M. W. Lo, J. E. Marsden, K. Padberg, R. Preis, S. D. Ross, and B. Thiere:' LTransport in dynamical astronomy and multibody problems , *International Journal of Bifurcation and Chaos in Applied Sciences and Engineering,*,2005

[**24**]G. Gomez, W. S. Koon, M. W. Lo, J. E. Marsden, J. Masdemont, and S. D. Ross:' Low energy transfer to the moon , *Celestial Mechanics and Dynamical Astronomy.*,2001

[**25**]M. W. Lo, W. S. Koon, J. E. Marsden, and S. D. Ross:' Connecting orbits and invariant manifolds in the spatial restricted three-body problem, *Nonlinearity*,15711606, 2004.

[**26**]Conley, C. C.:'On the ultimate behavior of orbits with respect to an unstable critical point. I. Oscillating, asymptotic, and capture orbits, *Journal of Differential Equations*,136-158, 1969

[**27**]Gomez, G., A. Jorba, J. J. Masdemont, and C. Simo:'A dynamical systems approach for the analysis of the SOHO mission' *International Symposium on Spacecraft Flight Dynamics*,pages 449-454, Germany,1991

[**28**]Farquhar, R. W.:'Future missions for Libration-point satellites, *Astronautics and Aeronautics,* 52-56,1969

[**29**]Gabern, F., W. S. Koon, and J. E. Marsden:' Spacecraft dynamics near a binary asteroid, *Discrete Dynamical Systems*,pages 297306, 2005

[**30**]Gomez, G., K. Howell, J. Masdemont, and C. Simo: Station keeping strategies for translunar libration point orbits, *AAS/AIAA Astrodynamics Specialist Conference,*,Paper No AAS 98-168, 1998

[**31**]Das A: *Solar Sail Trajectory Design in the earth moon circular restricted three body problem*,M.S. Thesis, Purdue University 2014

[**32**]Farquhar, R. W:' A halo-orbit Lunar station, *Astronautics and Aero- nautics,*,5963, 1972.

[**33**]J. E. Marsden and S. D. Ross:' New methods in celestial mechanics and mission design, *American Mathematical Society. Bulletin*,4373, 2006.

[**34**] Anna sama camo: Equilibria in three body problem: stability, invariant tori and connections, *Department of mathematics*, Barcelona, 2004.

[**35**]J. E. Prussing and B. A. Conway:, *Orbital Mechanics*,Oxford University Press,1993

[**36**]Petropoulos, A., Longuski, J., Bonfiglio:' Trajectories to Jupiter vio Gravity Assists from Venus, Earth, Mars , *AIAA Space Flight Mechanics Meeting*,November 2006

[**37**]E. A. Belbruno: *Capture dynamics and chaotic motions in celestial mechanics.* Princeton University Press, Princeton, NJ, 2004

[**38**]Abraham, R. and J. E. Marsden: *Foundations of Mechanics*,Originally published in 1967; second edition, 1978; the updated 1985 version reprinted by AMS-Chelsea in 2008, second edition.

[**39**]R. Jehn, S. Campagnola, D. Garcia, and S. Kemble:' Low-thrust approach and gravitational capture at mercury , *18th International Symposium on Space Flight Dynamics,*,November 2004

[**40**]M. W. Lo, W. S. Koon, J. E. Marsden, and S. D. Ross:' Low energy transfer to the moon , *Celestial Mechanics and Dynamical Astronomy.*,2001

[**41**]E. Canalias, G. Gomez, M. Marcote, and J. J. Masdemont:' Assessment of mission design including utilization of libration points and weak stability boundaries, European Space Agency, 2004.

[**42**]K. C. Howell, B. T. Barden, and M. W. Lo:'Application of dynamical systems theory to trajectory design for a libration point mission, *American Astronautical Society. Journal of the Astronautical Sciences,*,161178, 1997.

[**43**]M. W. Lo.:' Libration point trajectory design, Dynamical numerical analysis (Atlanta, GA, 1995).

[**44**]E. A. Belbruno and J. K. Miller:' Sun-perturbed earth-to-moon transfers with ballistic capture, *Journal of Guidance Control Dynamics*,pages 9597, New Jersey, 2003

[**45**]D. Folta and M. Beckman:' Libration orbit mission design: Applications of numerical and dynamical methods, *Proceedings of the Conference Libration Point Orbits and Ap- plications*,15711606, 2004.

[**46**]J. B. Marion and S. T. Thornton: *Classical Dynamics of Particles and Systems*,Saunders College Publishing, Fort Worth, 1995.

[**47**]K. C. Howell:' Three-dimensional, periodic, halo orbits, *Celestial Mechanics*,5371, 1984.

[**48**]Farquhar, R. W. and A. A. Kamel:'Quasi-Periodic orbits about the translunar libration point, *Celestial Mechanics*,458-473., 1973.

[**49**]Farquhar, R. W., D. P. Muhonen, C. Newman, and H. Heuberger.:' The first libration point satellite, mission overview and flight history, *AAS/AIAA Astrodynamics Specialist Conference*,1979

[**50**]E. Farquhar, R. W., D. P. Muhonen, C. Newman, and H. Heuberger:' Trajectories and orbital maneuvers for the first libration-point satellite, *Journal of Guidance and Control*,pages 549-554, 1980

[**51**]D.Gomez, G., A. Jorba, J. Masdemont, and C. Simo:' Study of the transfer between halo orbits, *Acta Astronautica*,493-520, 1998.

[**52**]Belbruno, E.:'*Capture Dynamics and Chaotic Motions in Celestial Mechanics: With Applications to the Construction of Low Energy Transfers*,Princeton University Press 2004

[**53**]Howell, K. C. and S. C. Gordon:' Orbit determination error analysis and a station-keeping strategy for Sun-Earth L1 libration point orbits' *The Journal of the Astronautical Sciences*,207-228, 1994.

[**54**]Llibre, J., R. Martinez, and C. Simo:' Transversality of the invariant manifolds associated to the Lyapunov family of periodic orbits near L2 in the restricted three-body problem, *Journal of Differential Equations.*,104-156, 1985

[**55**]Mains, D. L: *Transfer Trajectories from Earth Parking Orbits to L1 Halo Orbits*,M.S. Thesis, Purdue University 1993

[**56**]Marchal, C:' The Three-Body Problem, *Elsevier*,1990.

[**57**]Sood R: *Solar Sail Trajectory Application for mission design from the perspective of circular restricted three body problem*,M.S. Thesis, Purdue University 2014